THE ASTROPHYSICAL JOURNAL, 324:441–465, 1988 January 1

IMPROVED METHODS FOR THE MEASUREMENT AND ANALYSIS OF STELLAR MAGNETIC FIELDS

STEVEN H. SAAR[1]
Joint Institute for Laboratory Astrophysics, University of Colorado and the National Bureau of Standards
Received 1987 March 30; accepted 1987 May 27

ABSTRACT

I present several improved methods for the measurement of magnetic fields on cool stars which take into account simple radiative transfer effects and the exact Zeeman patterns. Using these methods, high-resolution, low-noise data can be fitted with theoretical line profiles to determine the mean magnetic field strength in stellar active regions and a model-dependent fraction of the stellar surface (filling factor) covered by these regions. Random errors in the derived field strength and filling factor are parameterized in terms of signal-to-noise ratio, wavelength, spectral resolution, stellar rotation rate, and the magnetic parameters themselves. Weak line blends, if left uncorrected, can have significant systematic effects on the derived magnetic parameters, and thus several methods are developed to compensate partially for them. The magnetic parameters determined by previous methods likely have systematic errors because of such line blends (particularly at later spectral types) and because of line saturation effects. Other sources of systematic error are explored in detail. These sources of error currently make it difficult to determine the magnetic parameters of individual stars to better than about $\pm 20\%$.

Subject headings: stars: late-type — stars: magnetic

I. INTRODUCTION

Magnetic fields play a central role in the atmospheric properties of late-type stars, and in the evolution of their "activity" (e.g., Linsky 1983, 1985; Haisch 1983; Soderblom 1983; Rosner, Golub, and Vaiana 1985; Zwaan 1986). Detailed confirmation and refinement of stellar activity theories therefore require information on the actual strength and extent of magnetic fields on stellar surfaces. Unfortunately, such data have been very difficult to obtain, partly because of inadequate observational techniques. All attempts to measure magnetic fields on late-type stars prior to 1980 analyzed polarized light (Babcock 1958). Results of these efforts have been inconclusive (e.g., Vogt 1980; Brown and Landstreet 1981), most likely owing to complex magnetic topologies. Like the Sun, late-type stars probably possess large numbers of bipolar magnetic regions (Borra, Edwards, and Mayor 1984), and since the vector sum of the many oppositely directed field elements on an unresolved stellar surface is then nearly zero, magnetographs detect an almost complete cancellation of the circular polarization signal. Any residual polarization is further diluted by unpolarized light from nonmagnetic regions of the stellar surface. Broad-band linear polarization does not cancel in integrated light, but is a much smaller effect and is difficult to interpret (Landi Degl'Innocenti 1982). Magnetic field detection techniques using polarized light thus are not very useful in studies of stars with solar-like magnetic geometries.

A major advance was made by Robinson (1980), who noted that the magnitude of the stellar vector magnetic fields could be derived from careful study in *unpolarized* light of the broadening of magnetically sensitive (high Landé g) line profiles. The method can determine both the average field strength in magnetic regions and the surface coverage (filling factor) of these regions, since line splitting is proportional to the field strength, and the relative intensities of the central and Zeeman split components in the profile can provide information on the filling factor. Because the Zeeman splitting is generally less than the intrinsic line width, Robinson proposed using a low–Landé g line formed at a similar level in the stellar atmosphere to deconvolve the magnetic parameters from a high-g line by rotationally broadening the profiles in Fourier space. This "Fourier ratio method" was first used by Robinson, Worden, and Harvey (1980, hereafter RWH) to measure magnetic fields on the active dwarf ξ Boo A. Several conceptually similar analysis schemes have been developed since (Marcy 1982; Giampapa, Golub, and Worden 1983, hereafter GGW; Gray 1984*a*) and applied to detect magnetic fields on about 25 late-type stars.

Recently, however, the Zeeman analysis methods have been criticized by several authors (Kurucz and Hartmann 1984; Gray 1984*a*; Giampapa 1984*a*; Gondoin, Giampapa, and Bookbinder 1985, hereafter GGB; Linsky 1985). The objections are varied, but they center on two flaws in the existing techniques: (1) the incomplete treatment of radiative transfer and (2) lack of correction for line blends. Indeed, on the basis of these objections, even the reality of magnetic line broadening detection has been called into question (Kurucz and Hartmann 1984).

In view of these problems, and of the importance of accurate magnetic field measurements to stellar physics, I have developed a new Zeeman analysis technique that is based on a simple radiative transfer model and includes compensation for blends. Here, I outline the general model and its application to the determination of stellar magnetic properties. I also investigate the reliability of stellar magnetic measurements through a thorough error analysis.

II. THE MODEL

a) Motivation

While line saturation effects in the individual thermal components of the split line profiles are incorporated in some tech-

[1] Guest Observer, National Optical Astronomy Observatories, which is operated by Associated Universities for Research in Astronomy, Inc., under contract to the National Science Foundation.

niques (Marcy and Bruning 1984; Gray 1984*a*), all previous methods of stellar analysis ignore the saturation effects arising from the Zeeman broadening itself. Previous techniques assume that a magnetically split line profile, $F_m(\lambda)$, can be represented by the weighted convolution of three unsplit line profiles, $F_0(\lambda)$. For a stellar atmosphere in which magnetic regions, identical to those arising from the unmagnetized areas but for the presence of a field, cover some fraction (filling factor) f of the surface, a high-g line profile, $F(\lambda)$, is modeled as

$$F(\lambda) = fF_m(\lambda) + (1-f)F_0(\lambda) = (1-f)F_0(\lambda) + fF_0(\lambda) * \left[\frac{A'}{2}\delta(\lambda - \Delta\lambda_B) + \frac{A'}{2}\delta(\lambda + \Delta\lambda_B) + B'\delta(\lambda)\right], \quad (1)$$

where $*$ indicates a convolution, δ is the Dirac delta function, A' and B' are weighting factors depending on the angle γ of the field lines to the line of sight, and $\Delta\lambda_B$ is the magnetic splitting. The weighting factors are (Babcock 1949)

$$A' = \tfrac{1}{2}(1 + \cos^2\gamma), \quad B' = \tfrac{1}{2}\sin^2\gamma, \quad (2)$$

and $\Delta\lambda_B$ is given by

$$\Delta\lambda_B = 4.667 \times 10^{-12} g_{\rm eff}\lambda_0^2 B. \quad (3)$$

Here, λ_0 is the line-center wavelength in nanometers, B is the magnetic field strength in gauss, and $g_{\rm eff}$ is the effective Landé g value of the transition, defined by (Beckers 1969)

$$g_{\rm eff} = \tfrac{1}{2}(g_u + g_l) + \tfrac{1}{2}(J_u - J_l)(g_u - g_l)(J_u + J_l + 1), \quad (4)$$

where g and J are the Landé g factors and angular momentum quantum numbers for the upper (u) and lower (l) levels. The selection of a suitable nonmagnetic $F_0(\lambda)$ profile is critical. In practice, the reference line chosen to approximate $F_0(\lambda)$ may be either a low Landé g line from the same star (Robinson 1980; Marcy 1982; Sun, Giampapa, and Worden 1987, hereafter SGW), the same high-g line in a presumed magnetically inactive star (GGW), or a profile derived from a model atmosphere (Gray 1984*a*). The "triplet convolution" assumption in equation (1), however, is imprecise, because the lines used in Zeeman analysis are not optically thin and they do not always have simple triplet splitting patterns.

The convolution assumption is strictly valid only when the lines are weak, that is, when the line-to-continuum opacity ratios are much less than unity ($\eta_0 = \kappa_l/\kappa_c \ll 1$). Most lines employed to date in solar Zeeman studies violate this condition to some degree. For K and M dwarfs, where lower $T_{\rm eff}$ strengthens many neutral metal lines, the problem becomes more severe. The fundamental difficulty is that even a slightly saturated line increases in equivalent width when broadened by the magnetic fields (Stepanov 1958), an effect the convolution assumption does not take into account. Users of previous methods must compensate by either selecting low-g comparison lines that are overly saturated compared with the "true" $F_0(\lambda)$ (RWH), by artificially scaling a weaker line by some means (Marcy 1984), or by generating model lines with excess opacity. These subtle effects can lead to systematic errors in the derived magnetic parameters. Equation (2) is also no longer valid when $\eta_0 > 1$ (Kjeldseth-Moe 1968).

The simple triplet assumption is accurate for modeling nontriplet lines only when $\Delta\lambda_B$ is small. (see Gray 1984*a*). When $\Delta\lambda_B$ is on the order of the Doppler width, significant deviations between observed and modeled profiles can occur. Note for example, the complex, clearly nontriplet line profiles seen in infrared spectra of AD Leo (see Fig. 1 of Saar and Linsky 1985).

A more important defect in previous magnetic modeling techniques is the neglect of the effect of line blends on the observed profiles. Depending on its strength and placement in a line profile, a specific blend can alter the derived magnetic field strength, the magnetic filling factor, or both (Marcy 1982; GGB). Previous methods (roughly in order of sophistication) select line pairs that appear blend-free in the solar spectrum (RWH; Marcy 1984) or in ratios of lines from stars of similar spectral types in Fourier space (GGW), or analyze large ensembles of lines to dilute statistically the effect of blends (Gray 1984*a*). Each method has drawbacks. First, it is doubtful that any line profile is free of blends at the $<1\%$ level, especially in stars cooler than the Sun. Second, Fourier ratios do not eliminate blends (GGB), since weak lines are additive to profiles to first order. Finally, statistical techniques rely on the relatively few lines with $g \gtrsim 1.5$ to discern typical Zeeman splittings (see Fig. 5 of Gray 1984*a*). Also, as I will show in § IV*b*, a *random* distribution of blends can produce *systematic* errors in the inferred f and B values. Existing techniques thus can only partly reduce the large systematic errors that line blends can cause in Zeeman analysis.

b) The Basic Model

The primary aims, therefore, in developing an improved method for stellar magnetic field analysis are to treat radiative transfer effects realistically, include the complete Zeeman patterns, and better compensate for blends in the line profiles. In addition, owing to the large number of variables in modeling Zeeman-split lines, the fitting procedure should be automated to remove personal bias from the process. These goals suggest a technique similar in spirit to that devised by Auer, Heasley, and House (1977, hereafter AHH) for the analysis of solar Stokes polarimetry, modified for stellar applications and including compensation for blends (Saar, Linsky, and Beckers 1986, hereafter SLB).

Following AHH, I assume that the lines are formed in local thermodynamic equilibrium (LTE). LTE has proved to be a good approximation in similar studies of the Sun (e.g., Beckers and Schröter 1968) and is probably reasonable for the weak- to intermediate-strength neutral metal lines used here (e.g., Lites and Cowley 1974). Magneto-optical effects (i.e., Faraday rotation or elliptical birefringence) may be ignored: although these can be important for the proper interpretation of solar Stokes polarimetry (Landolfi, Landi Degl'Innocenti, and Arena 1984, hereafter LLA), theory suggests that they are at best a fourth-order contribution to the unpolarized I component of the Stokes vector (Landi Degl'Innocenti and Landi Degl'Innocenti 1973). Tests by Landolfi and Landi Degl'Innocenti (1982), AHH, LLA among others have verified that Faraday rotation is not important in modeling unpolarized line profiles. The Hanle effect (line-crossing interference) may also be neglected, since the splitting due to typical (kilogauss) stellar magnetic fields will be much larger than the natural line width (Lamb 1970). *LS* coupling should hold for most of the lines (Solanki and Stenflo 1985), and hyperfine structure can be safely neglected by selecting lines from elements with small nuclear spin. Under these conditions, the equation of transfer for polarized light can be written in terms of opposite elliptically polarized components (Stepanov 1958):

$$\mu\frac{dI_\pm}{d\tau} = (1 + \eta_\pm)\left(I_\pm - \frac{B_\lambda}{2}\right), \quad (5)$$

where $I_\pm$ and $\eta_\pm$ are the specific intensities and absorption coefficients for right (+) and left (−) elliptically polarized light,

and B_λ is the source (Planck) function. This formulation is slightly more compact than the normal Unno (1956) formulation for the Stokes parameters I, Q, U, and V, and it has been shown to be equivalent by Rachkovskii (1961). The absorption coefficients are given by (note the misprint in SLB)

$$\eta_\pm = \tfrac{1}{2}[\eta_p - \tfrac{1}{2}(\eta_r + \eta_b)] \sin^2 \gamma + \tfrac{1}{2}(\eta_r + \eta_b) \pm \tfrac{1}{2}\{[\eta_p - \tfrac{1}{2}(\eta_r + \eta_b)]^2 \sin^4 \gamma + (\eta_r - \eta_b)^2 \cos^2 \gamma\}^{1/2} , \quad (6)$$

where γ is the angle between the line of sight and the magnetic vector and η_p, η_b, η_r are the line opacity functions for the π, blueshifted, and redshifted magnetic σ components, respectively. If η_0 is the line-to-continuum opacity ratio and ϕ is the line absorption function, which depends on the Doppler width $\Delta\lambda_D = (\lambda_0/c)(2kT/m + \xi^2)^{1/2}$ (where ξ is the Gaussian microturbulent velocity), the magnetic splitting $\Delta\lambda_B$, and, for strong lines, the Voigt parameter α, the line opacity functions are given by (e.g., Stepanov 1960)

$$\eta_p = \sum_{-n}^{n} \eta_{\pi i}\, \phi[\lambda \pm \Delta\lambda_B(g_{\pi i})] , \quad (7)$$

$$\eta_b = \sum_{1}^{m} \eta_{\sigma i}\, \phi[\lambda + \Delta\lambda_B(g_{\sigma i})] ,$$

$$\eta_r = \sum_{1}^{m} \eta_{\sigma i}\, \phi[\lambda - \Delta\lambda_B(g_{\sigma i})] , \quad (8)$$

with

$$\eta_0 \equiv \sum_{-n}^{n} \eta_{\pi i} \equiv \sum_{1}^{m} \eta_{\sigma i} . \quad (9)$$

Here, n is the smaller of J_u and J_l, with $m = 2n$ for even multiplicity and $m = 2n + 1$ for odd multiplicity. In the case of a simple triplet, equations (8), (9), and (10) reduce to the familiar $\eta_p = \eta_0\, \phi(\lambda)$, $\eta_b = \eta_0\, \phi(\lambda + \Delta\lambda_B)$, and $\eta_r = \eta_0\, \phi(\lambda - \Delta\lambda_B)$. The relative η_i and g_i are tabulated by Beckers (1969) for the case of pure LS coupling.

I assume a Milne-Eddington atmosphere with a source function linear in optical depth ($S_\lambda = B_\lambda = a + b\tau$, where B_λ is the Planck function). This atmosphere has been used successfully to model solar Stokes profiles by AHH, LLA, and Skumanich, Rees, and Lites (1984), among others. These authors find that the differences in the derived magnetic field strengths using more sophisticated model atmospheres are very small ($< 5\%$), since commonly used lines are relatively insensitive to the precise run of temperature with τ. On the other hand, if a strong gradient of the magnetic field exists in the line-forming region, an analysis using a Milne-Eddington atmosphere will yield an ill-defined "average" value of the field strength corresponding to some "mean" optical depth. Examples of the results for various functional forms of $B_\lambda(\tau)$ are given by LLA and AHH. Since the Milne-Eddington atmosphere works well for the Sun, however, height gradients in the field very likely do not alter the profiles significantly. I assume that this also is the case in other late-type stars. The magnetic transfer equations then have simple analytic solutions, and the emergent unpolarized specific intensity from a magnetic portion of a stellar atmosphere at a position angle μ is given by

$$I_m(\mu) = a + \frac{1}{2}\, b\mu\left(\frac{1}{1+\eta_+} + \frac{1}{1+\eta_-}\right) . \quad (10)$$

The unpolarized intensity arising from quiet, nonmagnetic portions of the stellar atmosphere, within the same set of assumptions, may be written as

$$I_q(\mu) = a' + b'\mu\left(\frac{1}{1+\eta'}\right) , \quad (11)$$

with $\eta' = \eta'_0\, \phi'(\lambda)$, ϕ' depending on $\Delta\lambda'_D = (\lambda_0/c)(2kT'/m + \xi'^2)$ and α.

If detailed spatial information is available from either direct observation (i.e., the Sun; see also Soderblom 1985), spectral modeling such as Doppler imaging (Vogt and Penrod 1983 for spot positions and areas, and Walter *et al.* 1987 for plages), or photometric studies (e.g., Eaton and Hall 1979), one can construct disk-integrated models using the above specific intensity functions for each point on the stellar surface. Unfortunately, very few stars other than the Sun have been studied in sufficient detail to warrant such a modeling effort, and knowledge of the differences in the atmospheric structures between magnetic and quiet regions on stellar surfaces (i.e., the primed and unprimed variables) is almost totally lacking. We thus are forced to model magnetic lines using a more simplistic approach. The effects of these simplifying assumptions will be explored in detail in § IV*b*.

To begin, I assume that uniformly distributed magnetic regions cover a fraction f of each model cell on the stellar surface. The specific intensity at any μ, normalized to the continuum ($I_c = a + b\mu$), is then given by

$$I(\mu) = \frac{fR_m}{fR_m + (1-f)} \frac{1 + (1/2)\beta\mu[1/(1+\eta_+) + 1/(1+\eta_-)]}{1+\beta\mu} + \frac{1-f}{fR_m + (1-f)} \frac{1 + \beta'\mu[1/(1+\eta')]}{1+\beta'\mu} , \quad (12)$$

where $\beta = b/a$, $\beta' = b'/a'$, and $R_m = (1+\beta\mu)/(1+\beta'\mu)$ is the magnetic-to-quiet continuum brightness ratio. To obtain the computed stellar flux to be compared with observations, a particular $I(\mu)$ is chosen to closely approximate the disk-averaged $I(\mu)$, and equation (12) is convolved with rotational $[v(\lambda)]$ and radial-tangential macroturbulent $[m(\lambda)]$ broadening functions (Gray 1976, 1978) and with the instrumental profile $[i(\lambda)]$. The resulting function,

$$F(\lambda) = I(\mu) * v(\lambda) * m(\lambda) * i(\lambda) , \quad (13)$$

represents a line profile from a rotating star that is uniformly covered by magnetic regions occupying a fraction f of its surface area. To make this approximation, an assumption concerning the magnetic geometry must be made. Because the true field topology is unknown, I assume that the field is everywhere radial, and take γ to be a disk-averaged value, $\langle\gamma\rangle$, weighted by foreshortening and limb darkening (Marcy 1982). For a linear limb-darkening law,

$$\langle\gamma\rangle = \frac{\int \gamma \cos\gamma(1 - \epsilon + \epsilon\cos\gamma) \sin\gamma\, d\gamma d\phi}{\int \cos\gamma(1 - \epsilon + \epsilon\cos\gamma) \sin\gamma\, d\gamma d\phi} = \frac{0.3927 - 0.1705\epsilon}{0.5 - 0.1667\epsilon} . \quad (14)$$

One could, alternatively, angle-average the absorption coefficients (eq. [6]). Linear limb-darkening coefficients (ϵ) are taken from Wade and Rucinski (1985) or Al-Naimiy (1978) and are also applied to the rotational broadening function $[v(\lambda)]$. The model can, if the data warrant, accommodate more than one type of magnetic region (dark spots and bright network, for

example) with the inclusion of appropriate specific intensity functions and respective filling factors (f) and relative brightnesses (R). Since detailed information concerning the physical characteristics of stellar active regions is lacking, and predictive theories do not yet exist, I assume as a first approximation that the physical parameters of the magnetic and quiet line-forming regions are identical (i.e., that the primed and unprimed variables are equal). In this case, equation (13) can be reduced to the form used by SLB in their analysis of EQ Vir.

III. APPLICATIONS OF THE MODEL TO DATA

The model described in § II can be used to derive magnetic field information from stellar spectra in several ways that differ primarily in how well they compensate for line blending. Perhaps the simplest application of the model is a variation of Robinson's (1980) Fourier ratio method. High- and low-g lines from the same star are selected, normalized to the local continuum, transformed, and ratioed in the Fourier domain. The result can then be modeled with the function

$$\frac{F_{\rm hi}(s)}{F_{\rm lo}(s)} = \frac{I_{\rm hi}(s)v(s)m(s)i(s)}{I_{\rm lo}(s)v(s)m(s)i(s)} = \frac{I_{\rm hi}(s)}{I_{\rm lo}(s)}, \qquad (15)$$

where $F_{\rm hi}$ and $F_{\rm lo}$ are obtained from the Fourier transform of equation (13) and s is the Fourier frequency. The main advantage of this method is that it does not require any knowledge of v sin i or macroturbulence, ζ: the only free parameters are $\eta_{\rm hi}$, $\eta_{\rm lo}$, f, and B (ξ is assumed). Blends, however, are not treated by this procedure unless removed prior to transforming. One can model several line pairs and hope that the effects of the blends average out statistically, but the small number of lines with $g_{\rm eff} > 1.5$ renders this an uncertain procedure, as noted earlier. The "anti-Zeeman" broadening (low-g lines broader than high-g lines) sometimes seen by Gray (1984*a*) likely is due to blends.

One can also employ a modification of Marcy's (1982) technique and model profiles directly using $F(\lambda)$ from equation (13) (e.g., SLB; see also Marcy and Bruning 1984). Obvious blends can be removed directly by a number of means, such as replacement of the corrupted portion of a line by its mirror image across line center, or by the addition of further opacity terms, $\eta_{\rm blend}(\lambda)$, to the line absorption coefficient. A determination of the velocity broadening parameters is first undertaken (assuming $f = 0$) using a set of low-g ($g_{\rm eff} \lesssim 1.3$) lines to obtain reliable ζ and v sin i values. Profiles may be normalized to line center to eliminate β as a parameter (AHH; SLB). In general, ξ is allowed to vary to account for small differences in turbulence and collisional broadening between lines. The results may then be applied to model high-g lines with η_i, f, and B as free parameters. If the magnetic analysis shows that substantial magnetic flux is present, some iteration will be necessary to obtain the optimum velocity and magnetic field parameters. Weak unresolved blends still will affect the results of the analyses, however. Indeed, for the moderately strong lines typically selected to study Zeeman broadening, blends will preferentially affect the unsaturated wings of the line profiles, leading to systematic errors in both the magnetic and velocity broadening analyses.

One approach to reduce the effects of blends is to compare the same magnetically sensitive line in two stars, one of which is presumed to be magnetically inactive. The magnetic "null" star is selected by two criteria. First, the two stars must be of very similar spectral type so that the atmospheric conditions in which the lines form are nearly identical. This ensures that the line blending in the two stars will be as similar as possible. Slight logarithmic scaling of the spectrum should be applied to adjust for small differences, for example, in metallicity between the two stars (Marcy 1984). The second criterion is that the proxy magnetic activity indicators of the "null" star must be near the lower end of the empirical ranges: i.e., weak emission in Ca II H and K, X-rays, and ultraviolet lines, and a long rotation period. The Sun, for example, is an excellent magnetic null star for stars of spectral type G2 V and $B-V \approx 0.67$. It has a small Ca II flux (log $[R'(\rm H + K)] = -4.94$; Noyes *et al.* 1984), a low X-ray output ($L_x/L_{\rm bol} = 1.6 \times 10^{-7}$; Marcy 1984), weak ultraviolet line emission (Ayres, Marstad, and Linsky 1981), and a long rotational period for its spectral type ($P = 25.4$ days). Indeed, direct observation shows $f_\odot \leq 0.02$. Candidate "magnetic null" stars for other spectral types can be gleaned, for example, from the well-studied "old" stars of the Wilson Ca II survey, for which Ca II fluxes, periods, and often many other parameters are known. Taking $f = 0$ for putative null stars, of course, could lead to systematic errors. For carefully selected objects, however, the assumption of a negligible filling factor should be reasonably good (see § IV*a*).

In practice, low-g lines in both stars first are modeled to determine the velocity broadening parameters. Since the stars are of the same spectral type, ζ should generally be similar in both (Gray 1984*b*). The spectrum of the star with the smaller v sin i (normally the inactive one) then is broadened to match the rotation of the other by multiplying the Fourier transform of the more slowly rotating star's profile by the ratio of rotational function transforms, $v_{\rm hi}(s)/v_{\rm lo}(s)$, and subsequently performing an inverse transform. Occasionally, a Fourier filter (Brault and White 1971) is needed to suppress ringing from the deconvolution. Alternatively, but less accurately, the profile may simply be convolved with $v_{\rm hi}(\lambda)$ when $v_{\rm lo} \ll v_{\rm hi}$, or with a Gaussian (GGW) having a full width chosen to compensate for differences in nonmagnetic broadening. After these modifications, and any scaling necessary to compensate for opacity differences, the two line profiles should in principle be identical except for possible magnetic broadening.

The analysis can then proceed in a number of ways. A Fourier ratio can be performed and the result modeled as $F(s)/F_{\rm quiet}(s)$. Essentially an improved (including radiative transfer, etc.) version of the GGW interstar Fourier ratio technique, this method still suffers from incomplete removal of blends (see § II*a*). Residual blends manifest themselves by the superposition on the transform of cosine ripples of various amplitudes and phases (GGB). Thus, the procedure is only a modest improvement over the "improved Robinson" method described at the beginning of this section.

A better alternative is to *subtract* the two profiles in the wavelength domain and model the residual (SLB; Saar, Linsky, and Duncan 1986) with

$$D_{\rm model}(\lambda) = [I(\lambda) - I'_{\rm quiet}(\lambda)] * v(\lambda) * m(\lambda) * i(\lambda), \qquad (16)$$

where $I'_{\rm quiet}$ is the suitably scaled model of the quiet star line profile. Here, because weak blends are roughly additive to the line profile, they will be removed in the difference. Inadequacies of the model also are suppressed owing to the differential approach. Disadvantages of this "interstar differential" method (SLB) include the uncertainty as to whether $f_{\rm quiet} \approx 0$, whether the stars have sufficiently well-determined parameters, whether they are well matched in spectral type, and whether the differences have been properly adjusted for. Furthermore, a

higher signal-to-noise ratio (S/N) is desirable to suppress the increase in noise resulting from the subtraction procedure. Nevertheless, the major systematic errors introduced by blends (see §§ II*a* and IV*b*) clearly argue for the use of such blend suppression techniques, at least for the cooler stars for which molecular blends are important.

One procedure to remove many of the sources of error in the interstar differential approach is to compare the same line in two spectra of the *same* star. This approach is particularly useful when magnetic variability is to be studied, and when one of the two spectra has accurately known B and f values and thus can be used as a "standard." Probably the best way to obtain such a standard is to observe a star simultaneously in the optical and the infrared. High-resolution, low-noise spectra of high-g infrared lines will result in partially or fully resolved Zeeman patterns for $B \gtrsim 1000$ G and moderate $v \sin i$, since $\Delta\lambda_B/\Delta\lambda_D \propto \lambda$. Modeling these resolved Zeeman split profiles is straightforward and can be accurately performed even in rather blended spectra using simple, direct profile-fitting methods (Saar and Linsky 1985). These results define the magnetic parameters of the simultaneous optical spectrum, which now serves as a standard. Any other optical spectrum of the same star can be analyzed differentially with the standard using, for each line profile

$$D_{\text{model}}(\lambda) = [I(\lambda) - I_{\text{std}}(\lambda)] * v(\lambda) * m(\lambda) * i(\lambda) . \quad (17)$$

This "intrastar differential" approach is superior, since by using the same star, problems of scaling line strengths and velocities are eliminated, as well as the need to know the atmospheric and velocity parameters for two stars.

Finally, it should be possible to make a detailed synthesis of blends using, for example, the ATLAS codes and extensive atomic and molecular line lists compiled by Kurucz and collaborators (Avrett and Kurucz 1983). Careful fitting of a solar flux spectrum and some magnetic null stars for the wavelength interval of interest could be used to check the adopted identifications and opacities of the blends for a range of T_{eff}. The blend spectra then could be used to remove blends prior to Zeeman analysis by one of the simpler methods (direct profile or Fourier ratio fitting). This approach requires considerable advance calculation, but holds promise and is under investigation.

IV. TESTS, CHARACTERISTICS, AND ACCURACY OF THE TECHNIQUE

a) Tests of the Method and Comparisons with Previous Techniques

A number of tests can be performed to see how accurately the techniques outlined in §§ II and III are able to derive magnetic parameters from real spectra. I first analyzed the spectrum of a large sunspot umbra at $\mu = 0.82$, obseved with the McMath echelle/bare Reticon system (Smith and Jaksha 1984) on 1984 April 13. The 4 nm bandpass was centered near the $g = 2.5$ Fe I line at 617.33 nm used by Marcy (1981, 1984). After flat-fielding and supression of 4 point electronic noise by interpolating out the noise peak in Fourier space, the S/N in the continuum exceeds 500. The spectrograph configuration minimizes scattered light to less than a few percent, so no correction was applied. Wavelength calibration was accomplished using a Th-Ar lamp. The resolution is $r = 80{,}000$, with ~ 3.5 pixels per resolution element and 2.2×10^{-3} nm per pixel. I first analyzed the data using the multiline profile-fitting method assuming $v \sin i = 0$ and $\zeta = 3$ km s^{-1}. The high-g line at 617.33 nm ($g = 2.500$) was too severely blended to model accurately, largely because of blends from the $\gamma'(0, 0)$ band of TiO. Instead, the 615.16 nm (Fe I, $g = 1.833$) and 615.60 nm (Ca I, $g = 2.00$) lines were used (SLB). Profile fits (Fig. 1) yielded $B = 2950 \pm 100$ G and $f = 0.98 \pm 0.02$ (1 σ errors). Direct measurement of the splitting of the σ components in polarized light at the Pulkovo Solar Observatory in the USSR (1984) about half a day later indicate $B = 3050$ G, in reasonable agreement with our results.

A more definitive test can be made using stellar data obtained on 1985 December 20. On this date, simultaneous high-resolution spectra of the active K2 dwarf ϵ Eridani were taken with the McMath system and with the NOAO 4 m Fourier transform spectrometer (4 m FTS; Hall *et al.* 1979). The 4 m FTS spectrum covered a 200 cm^{-1} bandpass centered around 4500 cm^{-1} (2.23 μm). The raw FTS data were transformed, flat-fielded, and apodized, and the telluric lines were removed, as described by Saar and Linsky (1985). The processed infrared spectrum has a resolution of 40,000 and S/N = 150; the optical spectrum has S/N = 400. As can be seen in Figure 2, no magnetic splitting is visible in the ϵ Eri data. Further, there is no systematic trend in line-shape change with Landé g value, placing limits on the magnetic parameters. Specifically, if $B > 2000$ G, the depths of the components must be less than the noise level, or $f \lesssim 0.05$. If, on the other hand, the fields are small, $Bf^{0.5} \lesssim 400$. In either case, the infrared spectra indicate that ϵ Eri had little magnetic flux at the time of observation. I next analyzed the optical spectrum using the profile-fitting method and the SLB line set, excluding the 615.6 nm Ca I line, which is too weak in ϵ Eri. The results (see Fig. 3) are $B = 3450 \pm 70$ G and $f = 0.084 \pm 0.005$ using the 617.3 nm line, and $B = 0 \pm 1000$ G and $f = 0.0 \pm 0.2$ using 616.16 nm. These results not only (in the case of 617.3 nm) conflict with the infrared data but also disagree with each other, suggesting that substantial systematic effects are present.

Unresolved blends are the cause of the systematic error. The high-g 617.33 nm line of ϵ Eri was studied using several interstar differential analyses. The magnetic null stars, chosen from "old" stars from the Wilson (1978) survey, are given in Table 1. Available data on chromospheric and coronal emission and rotation periods (Table 1) indicate that all of these objects should be magnetically inactive. Marcy (1984) reported detections of magnetic fields in two stars from this list (40 Eri A and 61 Cyg A). There is reason to question these results, however: four FTS spectra of 61 Cyg A (1985 March and December; see Saar and Linsky 1985) and one of 40 Eri A (1985 December) show no evidence of substantial magnetic flux.

Initially, I made the interstar analyses for the 617.33 nm line using only the stars closest to ϵ Eri in spectral type: 107 Psc, HD 4628, and HD 16160. As expected, the K2 star HD 4628 yields results closest to those inferred from the FTS data (Table 2). The magnetic fluxes derived from the other stars are also small, implying that slight differences in spectral type between null and target stars do not drastically alter the results. Only when null stars of significantly different temperatures were used (40 Eri A and 61 Cyg A) did the derived f differ noticeably from zero. The negative filling factors for HD 16160 and 61 Cyg A indicate that their 617.33 nm lines are wider than ϵ Eri's after the correction for rotational broadening (probably because of increased strength of line blends), leading to a false detection of magnetic flux on these null stars. The analysis of

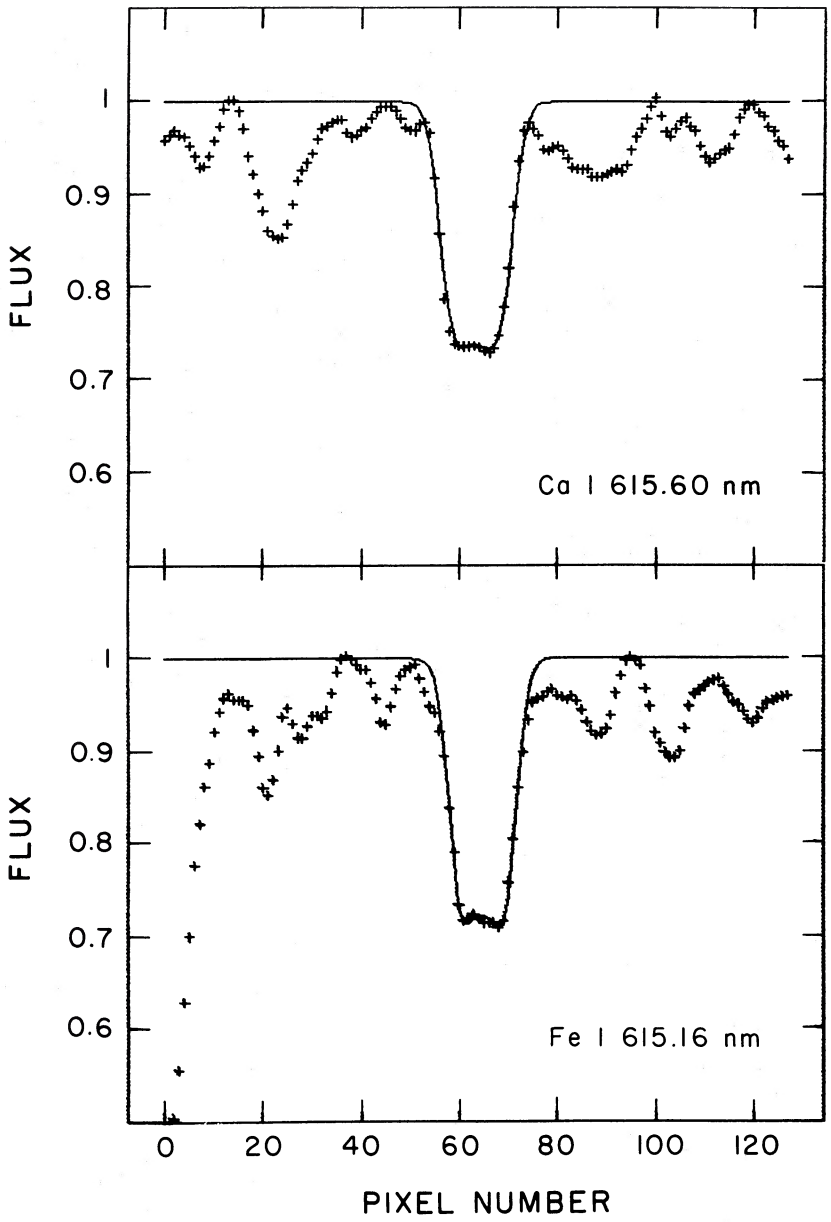

FIG. 1.—Profile fits to the 615.60 nm (Ca I, $g = 2.00$) and 615.16 nm (Fe I, $g = 1.833$) lines from a sunspot umbra. The derived magnetic parameters are $B \approx 2950 \pm 190$ G, and $f = 0.98 \pm 0.02$. Note the strong molecular line blending in the adjacent continuum. The scale of this McMath Reticon data is 2.2×10^{-3} pixel^{-1}, 3.5 pixels per resolution element.

TABLE 1

STELLAR PARAMETERS

Name	Spectral Type	$B-V$	P (days)	Ca II Flux Index $\langle S \rangle$	log L_x
Sun	G2 V	0.66	25.4	0.171	27.2
ξ UMa B	G5 V	~0.68	~4	0.445	29.3[a]
τ Ceti	G8 V	0.22	31.9	0.172	<27.6
HD 166	K0 V	0.75	~5.7	0.486	...
40 Eri A	K1 V	0.82	37.0	0.205	~27.7
107 Psc	K1 V	0.84	34.6	0.210	...
ϵ Eri	K2 V	0.88	11.3	0.510	28.3
HD 4628	K2 V	0.88	39.0	0.230	27.3
HD 16160	K3 V	0.98	45.0	0.230	...
61 Cyg A	K5 V	1.18	37.9	0.605	27.6

[a] Binary system. Relative contributions of the components to L_x are unknown.

the ϵ Eri data using 40 Eri A as a magnetic null is illustrated in Figure 4. Note that even intercomparing ϵ Eri with stars of spectral types as far removed as K0 V and K5 V (see Table 2) yields B and f values that are not much larger than the limits set by the infrared spectrum. The interstar differential approach therefore appears to be a viable method for deriving the magnetic parameters of late-type dwarfs when magnetic null stars are carefully selected.

I have also analyzed four spectra kindly provided by Dr. G. Marcy, using the profile approaches. The data, consisting of profiles of the 617.33 and 624.06 ($g = 1.00$) nm lines for each star, were taken at Lick Observatory and have a resolution of 10^5 with 1.48×10^{-3} nm per pixel and 4 pixels per resolution element. Following Marcy (1984), the continuum was defined locally. Marcy (1984) lists magnetic parameters derived from these spectra using his profile-addition technique (Marcy

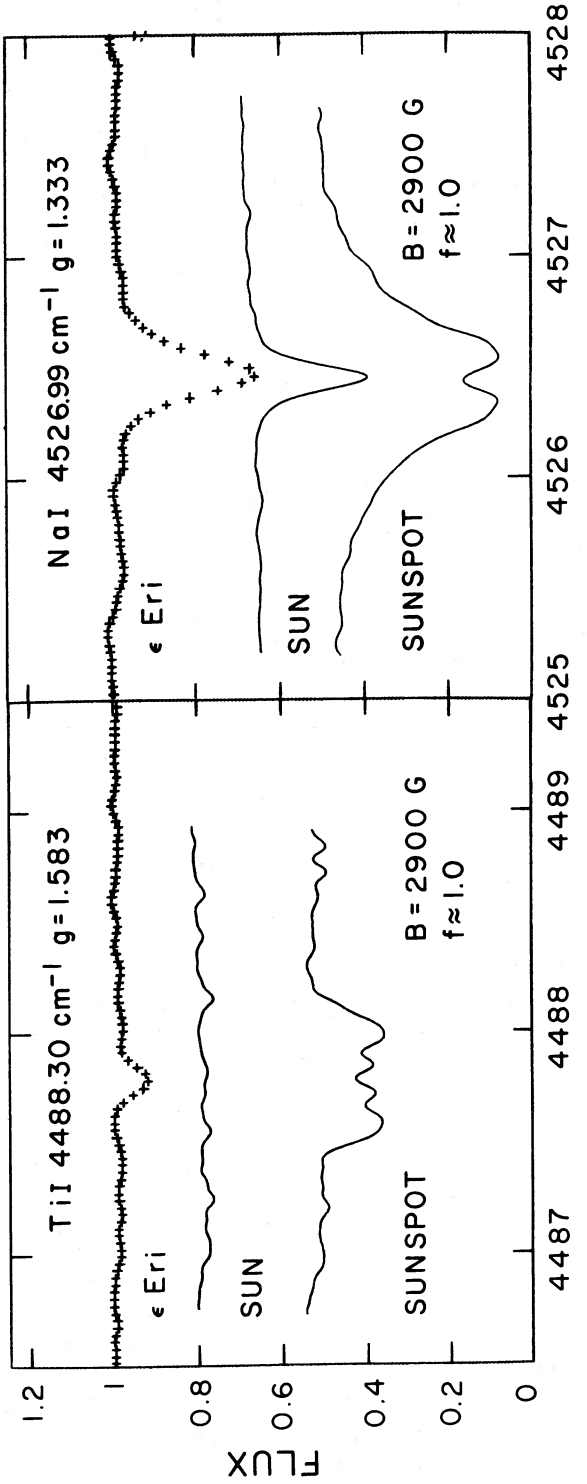

FIG. 2.—Four meter FTS data of the active K2 dwarf ε Eri, compared with profiles from the solar photosphere and umbrae from Hall's (1973) atlas. No Zeeman splitting or broadening is evident in the ε Eri data.

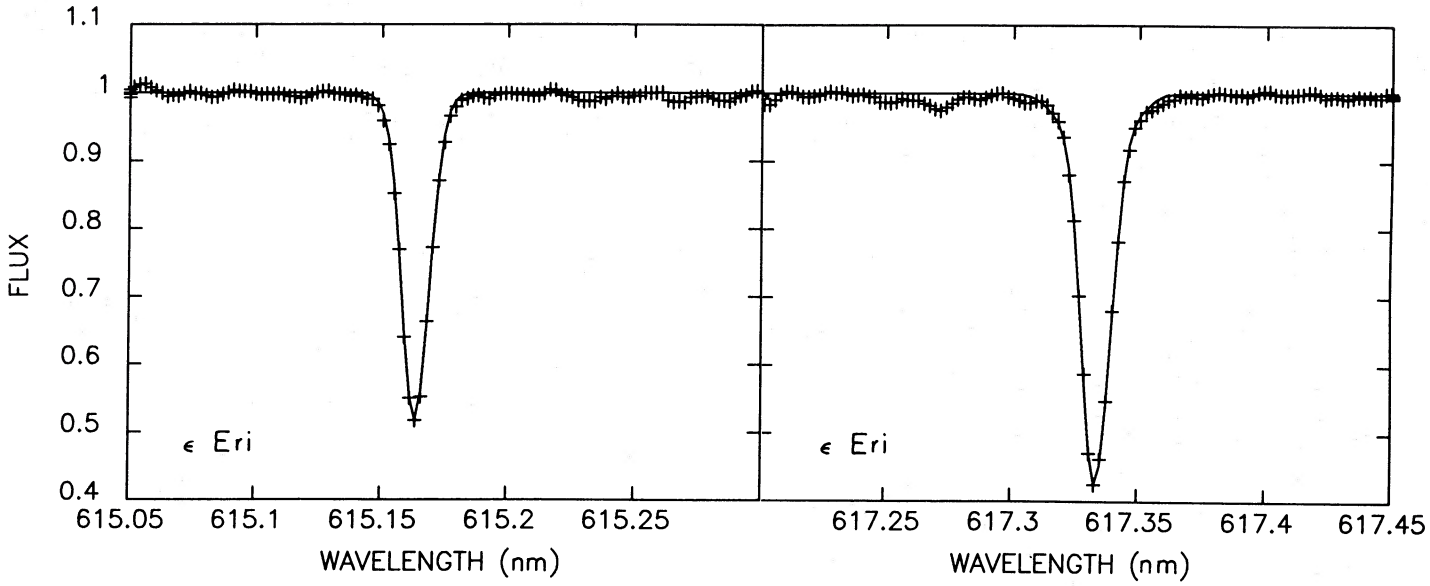

Fig. 3.—Profile fits to the 617.33 nm (Fe I, $g = 2.500$) and 615.16 nm (Fe I, $g = 1.833$) lines from ϵ Eri. The derived magnetic parameters are $B = 3450 \pm 70$, and $f = 0.084 \pm 0.005$ and $B = 0 \pm 1000$ G, $f = 0 \pm 0.10$, respectively. Parameters derived from these two lines from the same multiplet indicate that substantial systematic effects are present, likely due to line blends.

1982), which does not include radiative transfer or compensation for line-blending effects. This test therefore directly compares the results of the techniques developed here with those of Marcy. Results are presented in Figure 5 and Table 3. Good agreement is found for the spectra of ξ UMa B and τ Ceti: for these G stars, blends apparently are not significant and, since $\eta_0 \sim 1$, saturation effects are small. Magnetic parameters derived for the K stars HD 166 and 61 Cyg A, however, differ more significantly from Marcy's results, probably because of increased saturation effects in the K stars. Infrared FTS spectra of 61 Cyg A, as noted earlier, however, consistently show *no* evidence for magnetic broadening or splitting ($f \lesssim 0.05$ for $B > 2000$ G). An idea of the relative importance of blends and saturation in the 617.33 nm line, therefore, can be inferred from the differences between Marcy's result (with no treatment of saturation or blends), the profile modeling result (treating saturation only), and the FTS data. For the 617.33 nm line, blending clearly is significant.

b) Sources and Magnitudes of Systematic Error

A number of authors (Gray 1984*a*; Giampapa 1984*a*; Kurucz and Hartmann 1984; GGB; SLB; Linsky 1985) have argued that the neglect of line saturation and blends can be significant sources of systematic error in the inferred magnetic parameters, and in § IV*a* I presented strong confirming evidence. In this section, I investigate the extent of these and other systematic effects on previous methods and on those developed here.

TABLE 2

DIFFERENTIAL ANALYSIS OF λ617.3 nm IN ϵ ERI $fB \approx 0$ SPECTRUM WITH QUIET STARS

Comparison Object	B (G)	f	S/N of Difference Spectrum	$v \sin i$ (km s^{-1})
40 Eri A	2800 ± 700	$0.07^{+0.02}_{-0.01}$	175	1.0 ± 0.7
107 Psc	2800 ± 500	0.05 ± 0.01	250	1.1 ± 0.5
HD 4628	2950:	0.03	150	0.0 ± 1.0
HD 16160	5600:	−0.02:	150	1.0 ± 0.8
61 Cyg A	4400 ± 250	-0.11 ± 0.02	275:	1.3 ± 0.6

I first compared the Robinson (1980) Fourier ratio analysis with the procedure outlined in § III for lines with differing η_0. The ideal case is assumed: that is, both lines are free of blends, and the low-g or "null" line profile, $F_0(\lambda)$, is an exact representation of $F(\lambda)$ in the absence of a magnetic field. Line parameters of the model G star in Table 4 were assumed, with additional models calculated for $\eta_0 = 1$ and 20. The $F_0(\lambda)$ profile was scaled to the same equivalent width as $F(\lambda)$ using Marcy's (1984) logarithmic method. The two lines were then Fourier-transformed and ratioed, and the residual was modeled using the Robinson method (eq. [18]). The fitting procedure was terminated once the transform amplitude fell below that corresponding to S/N = 100 in the wavelength domain. Points in the Fourier ratio were weighted in proportion to the Fourier amplitude of the original lines at that frequency. An example of a Fourier ratio fit is displayed in Figure 6, and the resulting fractional deviations ($\delta_B \equiv B_{\rm fit} - B$, $\delta_f \equiv f_{\rm fit} - f$) of the Robinson fits from the models are depicted in Figure 7. The deviations have been scaled to constant line *depth* S/N (i.e., the $\eta_0 = 1$, 5, and 20 contour plots were divided by the square roots of 0.67, 0.36, and 0.30, respectively) to correct for the reduced magnetic parameter errors due to the larger S/N in the stronger lines. In this unbiased look at the neglect of line saturation effects in previous techniques, it is clear that for lines with $\eta_0 > 1$, the neglect of line saturation leads to *systematic errors*. The filling factor is most affected, *especially at low values*, because the increasingly square-shaped line profile produced by saturation is interpreted by the Robinson method as evidence for a large filling factor. Errors are less than 30%, however, for $B > 1500$ G and $1 < \eta_0 < 10$. Thus, as a first-order analysis *in the absence of significant line blends*, the simple Robinson (1980) approach is adequate in stars with *moderately strong fields*. Marcy's profile fitting and Gray's multiline Fourier approach will be similarly accurate.

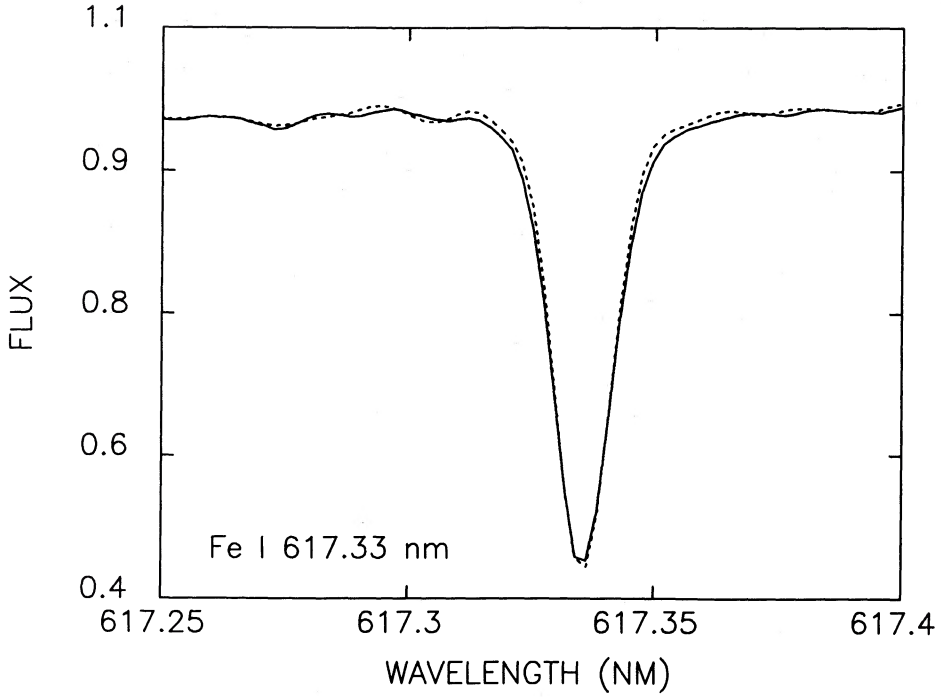

FIG. 4*a*

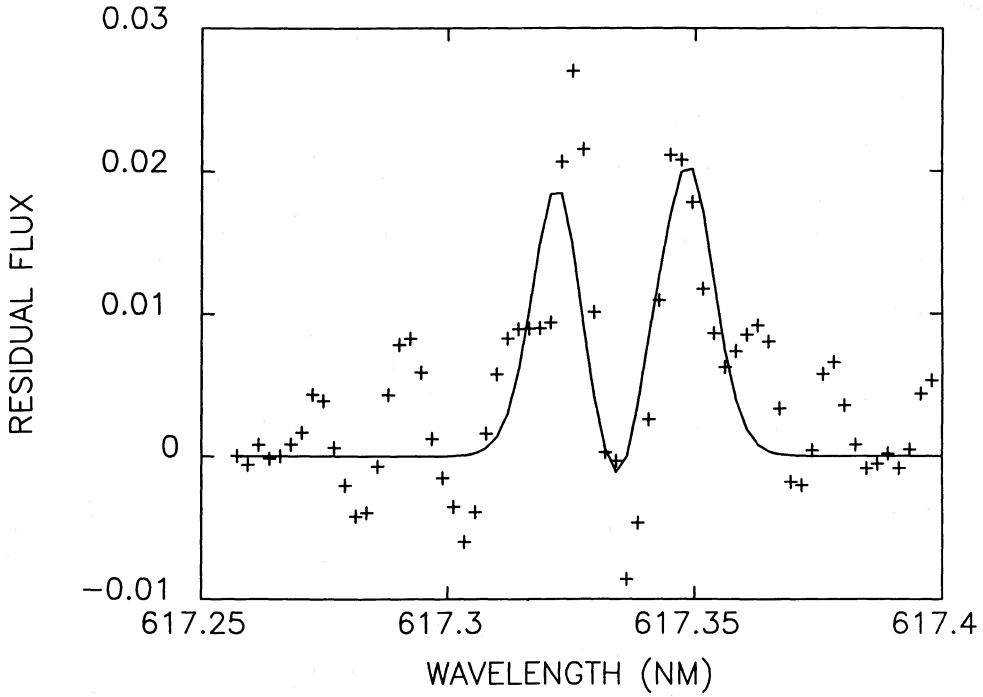

FIG. 4*b*

FIG. 4.—(*a*) Differential analysis comparing ϵ Eri (K2 V, *solid curve*) and 40 Eri A (K0 V; *dotted curve*) at 617.33 nm. The 40 Eri A profile has been logarithmically scaled to the same depth as the ϵ Eri profile. The 40 Eri A data have a slightly higher resolution and lower v sin i. Note that the scaling does not completely remove saturation differences between the stars. (*b*) Model (*solid curve*) to the difference of the two profiles in Fig. 4*a* (*plus signs*). Different saturation, v sin i, and resolution are all included in the model. The derived magnetic parameters are $B = 2800 \pm 700$ G, $f = 0.07 \pm 0.02$. This result is almost certainly due to blending, since simultaneous infrared spectra of ϵ Eri show no magnetic fields ($f \leq 0.05$) (see Fig. 2).

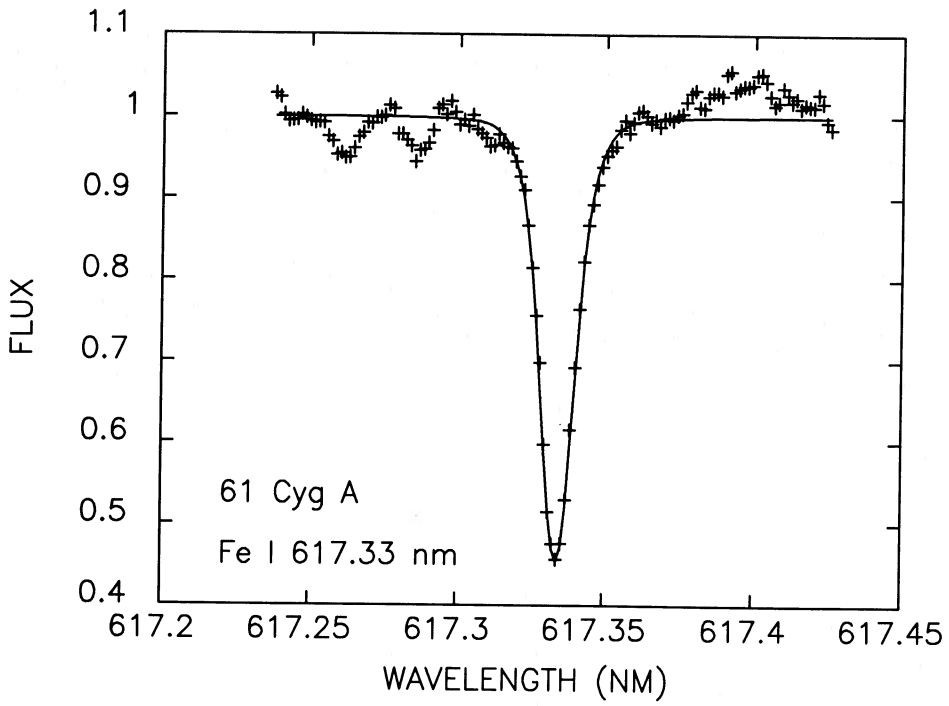

FIG. 5.—Profile fit to Marcy's 61 Cyg A data for the magnetic parameters $B = 3220 \pm 40$ G, $f = 0.16 \pm 0.01$. Marcy (1984) found $B = 2660$ G, $f = 0.30$. The greater discrepancy here is likely due to the larger line saturation in this cooler star. Marcy's models do not include line transfer effects.

As shown in § IV*a*, however, blends become significant (at least for 617.33 nm) at spectral type G8 V–K0 V, and the errors they can induce in f and B are far from negligible. Selection of another high-g line will probably not improve matters, since λ617.3 nm was specifically chosen as one of the most blend-free high-g lines in the optical spectrum (Robinson 1980; Marcy 1984). A study of commonly used high-g lines (Harvey 1973; Robinson 1980) in the Harvey (1977) sunspot atlas confirms this: the 525.0 nm line is rather strongly blended (and very temperature-sensitive—see Stenflo 1971); λ630.1 nm is blended by telluric and other lines; λ684.2 nm is blended by strong lines in both wings; and λ846.8 nm has a moderately strong feature in its redward wing. Thus, for stars of spectral type G8 V and later, it is essential to compensate for blends.

The blend removal methods developed here are, of course, approximate. The interstar differential approach, in particular, will be imperfect, since the null star cannot match the target star exactly, and differences in abundances and temperatures can alter the strengths of the blends. To obtain some insight into the possible systematic effects involved, blends with different strengths, $\eta_{\rm blend}$, were introduced at varying positions into theoretical (no noise) G and K star lines, and the resultant synthetic lines were modeled using the profile approach (eq. [13]), both directly and after averaging the line about line center. The resulting errors, given in Figure 8, show that incompletely removed blends are sources of systematic errors of the order of only 10% in f and B for the G star and 5% for the K star. Averaging around line center was found to increase errors, despite an improvement in the quality of the fit. The pattern of the deviations follows a predictable form. A blend near line center ($\Delta\lambda_{\rm blend} \lesssim \Delta\lambda_B/2$) contributes primarily to the unshifted, nonmagnetic portion of the profile, and this tends to *decrease* the measured filling factor. Blends positioned at $\Delta\lambda_B/2 < \Delta\lambda_{\rm blend} < \Delta\lambda_B$ from line center act to increase the filling factor and decrease the field strength, because they enhance the apparent depth of the magnetically split σ components while shifting their centroids closer to line center. Finally, blends located farther than $\pm\Delta\lambda_B$ from λ_0 bias the magnetic σ components toward larger values of B but progressively small values of f as the centroid of the magnetic σ component moves further from $\Delta\lambda_B$. A vertical cut (at constant $\eta_{\rm blend}$) shows this pattern clearly (Fig. 9).

I have also computed the effects of blends in theoretical $B = 0$ line profiles. This experiment, which parallels the

TABLE 3

REANALYSIS OF MARCY'S DATA

	MARCY		THIS WORK (no blend correction)			
STAR	B (G)	f	B (G)	f	$v \sin i$ (km s^{-1})	η_0 (for $\beta \equiv 12$)
ξ UMa B	1660	0.37	1970 ± 160	0.32 ± 0.04	2.3 ± 0.7	2.6
τ Cet	...	...	0	0	1.5 ± 0.9	2.3
HD 166	2250	0.41	3040 ± 250	0.30 ± 0.03	3.9 ± 0.5	16
61 Cyg A	2660	0.30	3220 ± 40	0.16 ± 0.01	1.9 ± 0.4	14

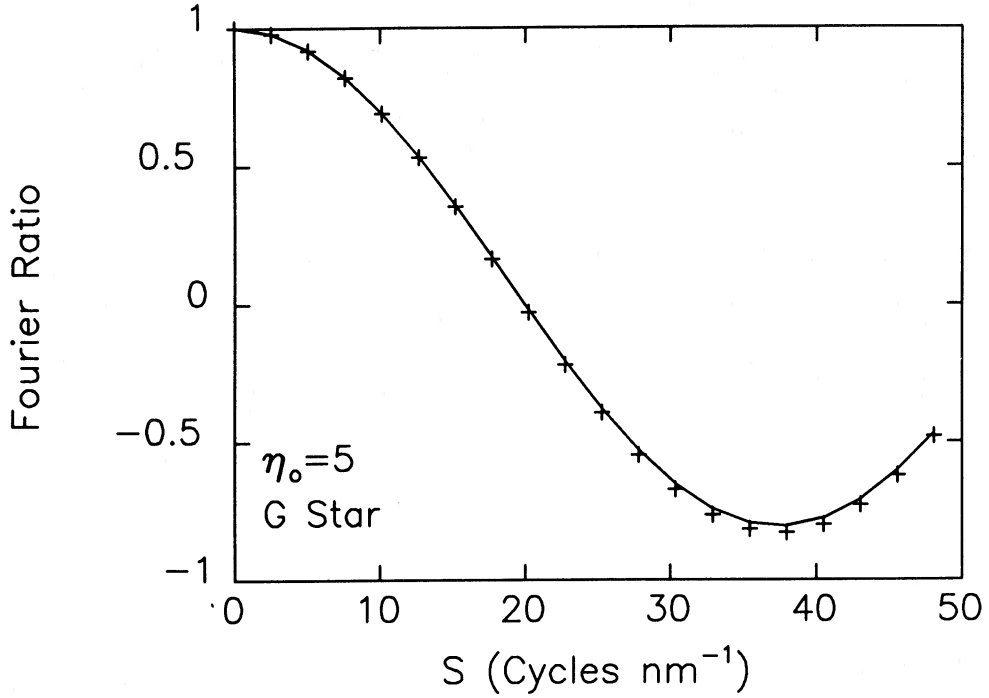

FIG. 6.—Fourier ratio (*plus signs*) of G star model with $B = 3000$ G, $f = 1.00$ and an identical model having $B = 0$. The solid line is a fit using the Robinson (1980) method, truncated at 23 cycles nm^{-1} (where the transform dips below S/N = 100). The derived parameters are $B = 3005$ G, $f = 1.157$, showing the systematic errors of the Robinson method due to lack of treatment of line transfer effects. The $B = 3000$ G and $B = 0$ lines were normalized to the same equivalent width before modeling.

analysis in § IV*a* of the ϵ Eri $fB \approx 0$ spectrum, probes errors resulting from the neglect of blends in nondifferential approaches, such as previous techniques and the profile and Fourier ratio approaches outlined here. I have analyzed the G star line with $B = 0$ as before, for the same range of $\Delta\lambda_{\rm blend}$ and $\eta_{\rm blend}$. Derived (spurious) magnetic parameters are given in Figure 10. Not surprisingly, the inferred magnetic splitting closely follows the blend position, with $\Delta\lambda_B = \Delta\lambda_{\rm blend}$. The inferred f value, on the other hand, is fairly constant at 0.1–0.2 for $\Delta\lambda_{\rm blend} > 0.003$ nm, increasing only somewhat with $\eta_{\rm blend}$. Below this splitting however, the apparent filling factors rapidly increase. *The large-f, low-B measurements frequently obtained by Marcy (1984) at later spectral types thus could have been due in part to blends near the core of* λ617.33 nm. Some candidate line blends are given in Kurucz and Hartmann (1984). Note that because of the uneven distribution of errors, the effect of a random distribution of blends of various strengths will *not* cancel out, even when large numbers of lines are modeled.

Errors in the determined or assumed nonmagnetic parameters also affect the filling factor and magnetic field measurements (SLB). I have reanalyzed noise-free G and K star lines using the profile method, and have introduced errors into selected nonmagnetic parameters (microturbulence, rotational velocity, and opacity; e.g., Fig. 11). It appears that for reasonable uncertainties in the nonmagnetic parameters, errors in the magnetic field and filling factor are moderate (less than 30%; see also SLB). Very generally, when a parameter is underestimated, the magnetic field is overestimated and the filling factor is decreased by an even larger amount. The reverse holds when a given nonmagnetic parameter is set at too high a value. The reason for this behavior is the smoothing effect of these parameters on the line profile. When ξ, $v \sin i$, or η is underestimated, the magnetic field strength must increase to compensate for the increased broadening needed to fit the line properly. Because the equivalent width has not changed, however, f must decrease in concert, so that, roughly, $Bf^{0.5}$ remains approximately constant. As expected, the lower B and f of the G star line model make it more sensitive to errors in the nonmagnetic parameters. Incorrect placement of the continuum level also can be a source of error in f and B. Again, the G star line with no noise was analyzed with the continuum purposely set within $\pm 2\%$ of the actual value. Figure 12 shows that this is a moderate contributor to the total error ($< \pm 20\%$).

Improper assumptions of the modeling techniques (§ II*b*) are additional sources of errors in f and B. I first investigated possible errors due to differences in the physical properties of magnetic regions. The Sun is our only guide in this respect. Observations of solar magnetic regions outside of spots (plages and network) support the assumption that the magnetic field regions are relatively homogeneous. Howard and Stenflow (1972) and Frazier and Stenflo (1972) found that 90% of the

TABLE 4

PARAMETERS FOR MODEL STAR LINE PROFILES

Name	B	f	λ_0	η_0	β	ϵ	$T_{\rm eff}$	$\langle\gamma\rangle$
G dwarf.....	1500	0.3	6173	5	12	0.6	5500	41.6
K dwarf.....	2500	0.5	6173	10	12	0.8	4250	40.1
M dwarf.....	3500	0.5	22400	10	4	0.4	3500	42.9

NOTE.—For all stars $\xi = 1$ km s^{-1}, $\zeta = 3$ km s^{-1}, $\lambda/\Delta\lambda = 10^5$, $v \sin i = 0$, $\alpha = 0$.

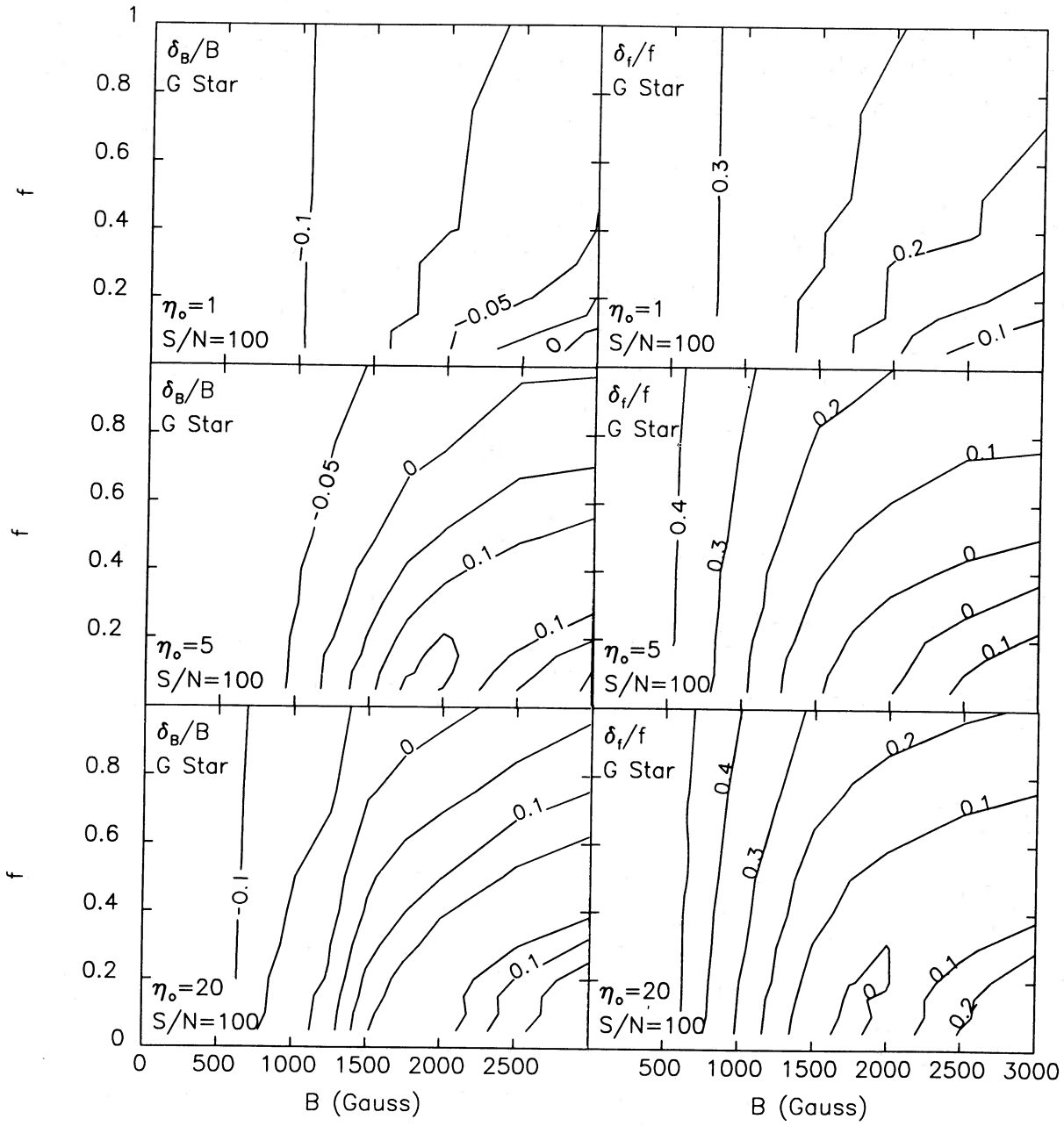

FIG. 7.—Map of normalized deviations, δ_B/B and δ_f/f, of the measured magnetic parameters from the actual values when analyzed using the Robinson technique (Fig. 6). The G star line parameters were used, with η_0 set at 1, 5, and 20, and S/N = 100. The results were scaled slightly to balance the decreased errors in stronger lines (see text).

solar magnetic flux exists as 1–2 kG flux tubes in plage and network. There is also evidence that these flux tubes may have fairly constant properties (Livingston and Harvey 1969), with field strengths nearly independent of their local number density or flux (Stenflo and Harvey 1985). The uniformity of field strength in solar plage and network has been confirmed by investigators using a variety of techniques (Beckers and Schröter 1968; Stenflo 1973; Harvey and Hall 1975; Tarbell and Title 1977; Wiehr 1978; Solanki and Stenflo 1984). The thermodynamic properties of the solar "bright" magnetic areas are more uncertain (cf. Frazier 1978; Solanki and Stenflo 1985), but it is generally believed that these regions are a few hundred degrees warmer than the quiet photosphere in the line-forming layers (Chapman 1977; Solanki and Stenflo 1984, 1985). Typical neutral metal lines formed in plage and network therefore weaken somewhat because of the higher temperature. For carefully selected lines that are relatively insensitive to temperature, however, the net contribution to the integrated stellar line profile is nearly identical with that for a line formed at the quiet region temperature. Furthermore, Doppler widths in the network and quiet areas are roughly the same (Stellmacher and Wiehr 1971).

Ca II H and K modulation studies (e.g., Noyes *et al.* 1984) and ultraviolet Doppler imaging (Walter *et al.* 1987) suggest

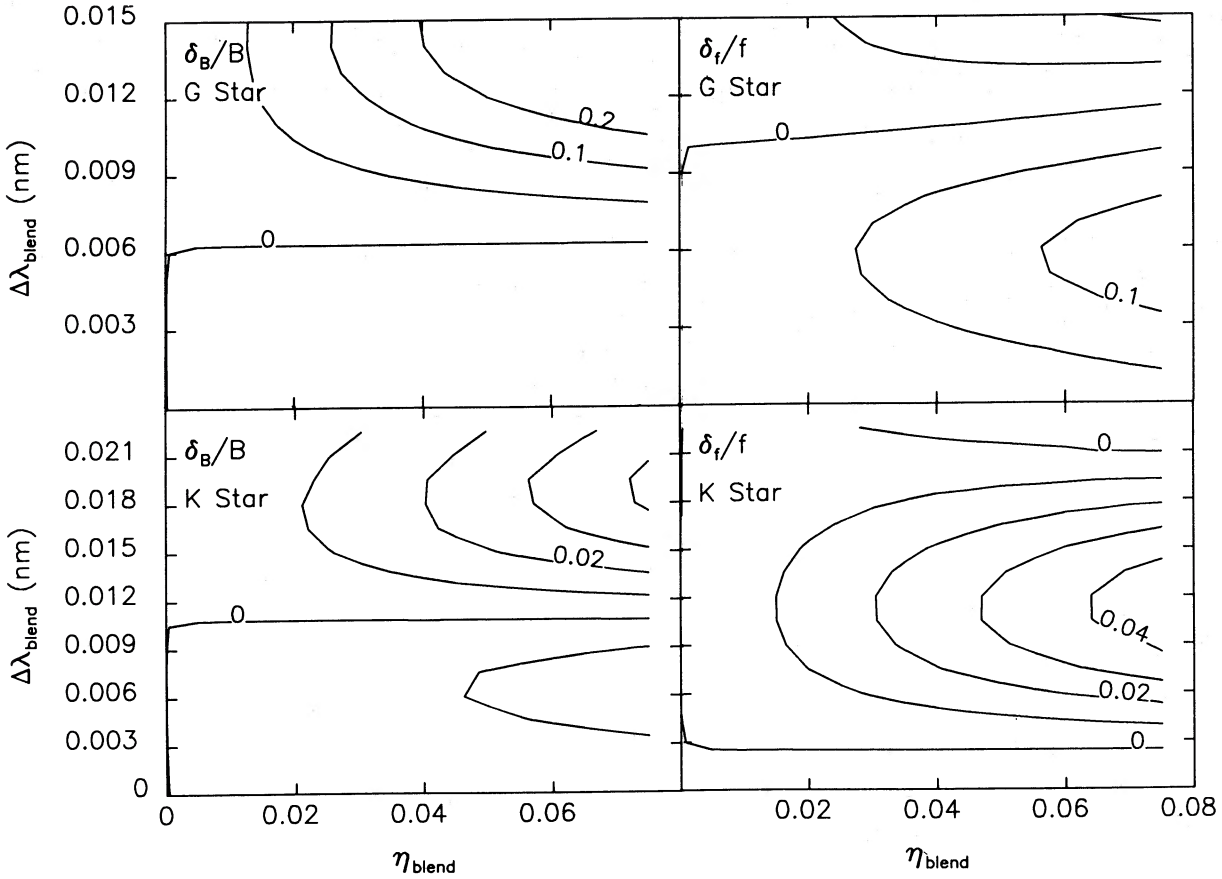

FIG. 8.—Deviations δ_B/B and δ_f/f caused by blends at various positions and strengths in the G (*top*) and K (*bottom*) star model lines.

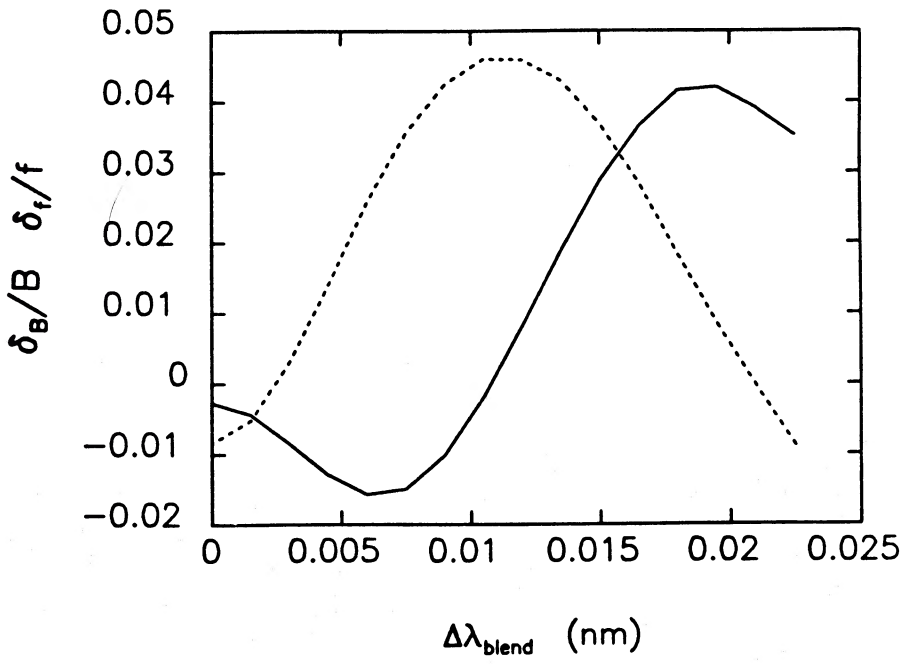

FIG. 9.—A cut through the K star contour plots in Fig. 8 at constant η_{blend} (= 0.08) showing the deviations δ_B/B (*solid curve*) and δ_f/f (*dotted curve*) as a function of $\Delta\lambda_{blend}$.

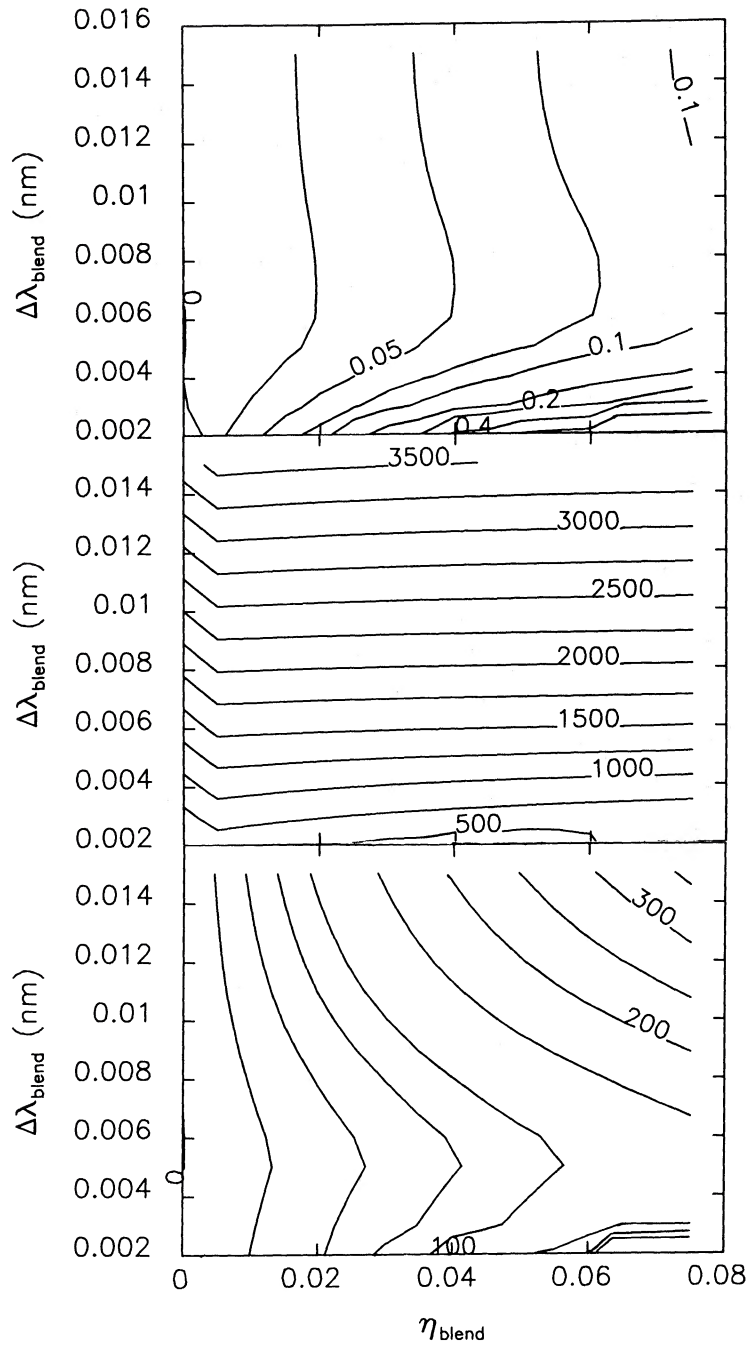

FIG. 10.—Map of the spurious filling factor (*top*), magnetic field (*middle*), and average field ($=fB$) when blends of strength η_{blend} are placed in the G star model with $B = 0$.

that plagelike structures exist on stars as well. Lacking any detailed information, the assumption made in § II that stellar plage regions are "solar-like" (i.e., with an optical continuum brightness ratio $R_m \approx 1$, a uniform field strength, and thermodynamic properties similar to the nonmagnetic stellar regions) seems a reasonable first approximation. Some effects of nonconstant field strengths are discussed by Gray (1984*a*). It should be stressed, however, that at least for the Sun, the range in field strengths in active regions is quite small; Stenflo and Harvey (1985) found $\Delta B = \pm 100$ G (SGW, however, find that B in newly emerging regions is smaller).

In sunspot umbrae, magnetic field strengths range from 2–3 kG (Allen 1976) and temperatures are about $0.7T_{phot}$. Similar values of T_{spot}/T_{phot} have been found on active stars through a combination of Doppler imaging and photometric modeling (Vogt 1983). For magnetic field measurements in the visual (600 nm) such temperatures imply brightness ratios of $R_{spot} = 0.20$; infrared measurements at 2000 nm would yield $R_{spot} = 0.70$. Typical active dwarfs have spot filling factors of $<5\%$ (Dorren and Guinan 1982; Campbell and Cayrel 1984), while BY Dra variables have $f_{spot} \approx 10\%$ (Rodonò *et al.* 1986), with up to 20% coverage in extreme cases (Poe and Eaton

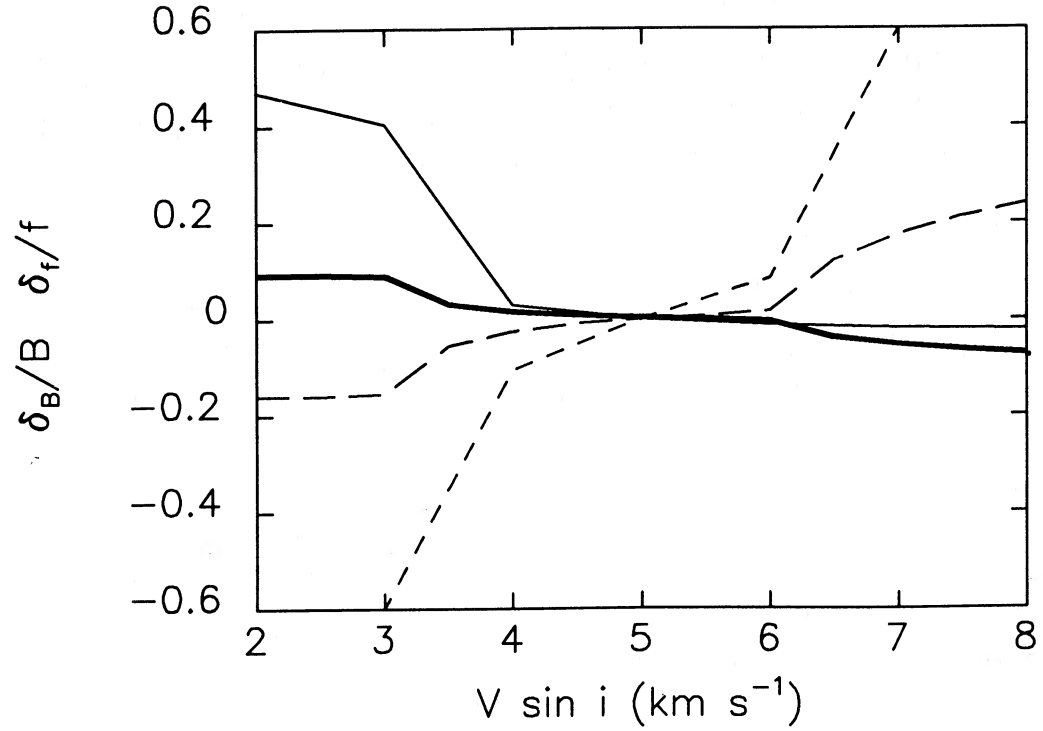

FIG. 11.—Deviations δ_B/B (*solid curve*: G star; *heavy solid curve:* K star) and δ_f/f (*dashed curve:* G star; *long-dashed curve:* K star) for the G and K star models with $v \sin i = 5$ km s^{-1} when different $v \sin i$ are used.

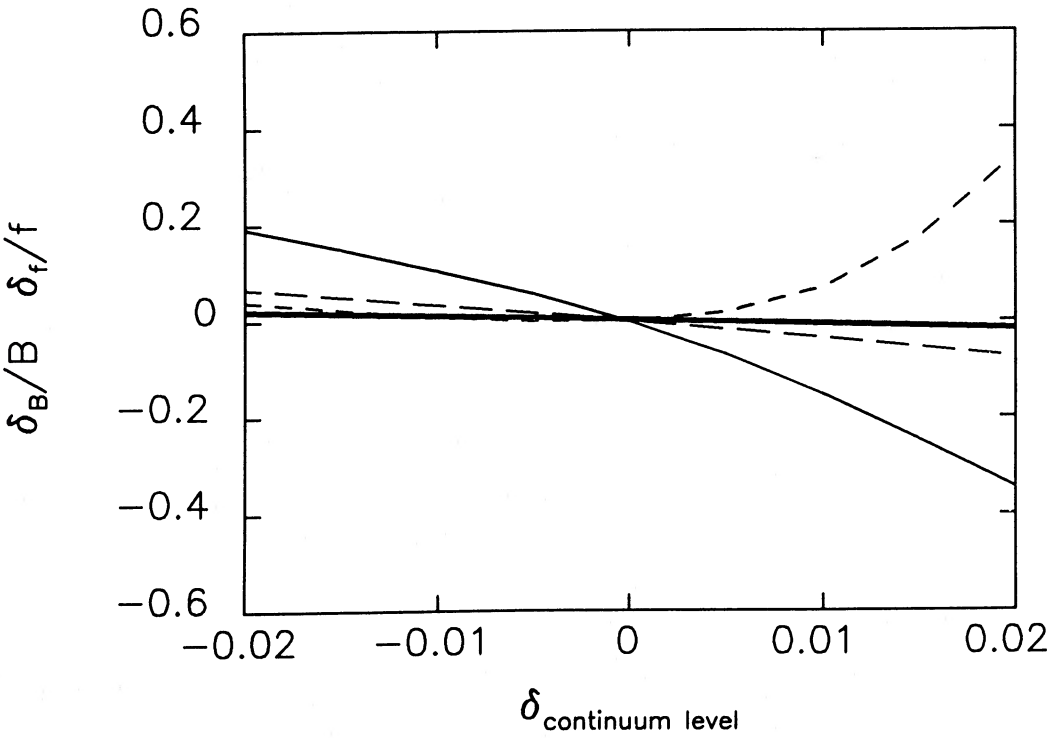

FIG. 12.—Deviations δ_B/B (*solid curve:* G star; *heavy solid curve:* K star) and δ_f/f (*dashed curve:* G star; *long-dashed curve:* K star) for the G and K star models when the continuum level is set within ± 0.02 of the actual value.

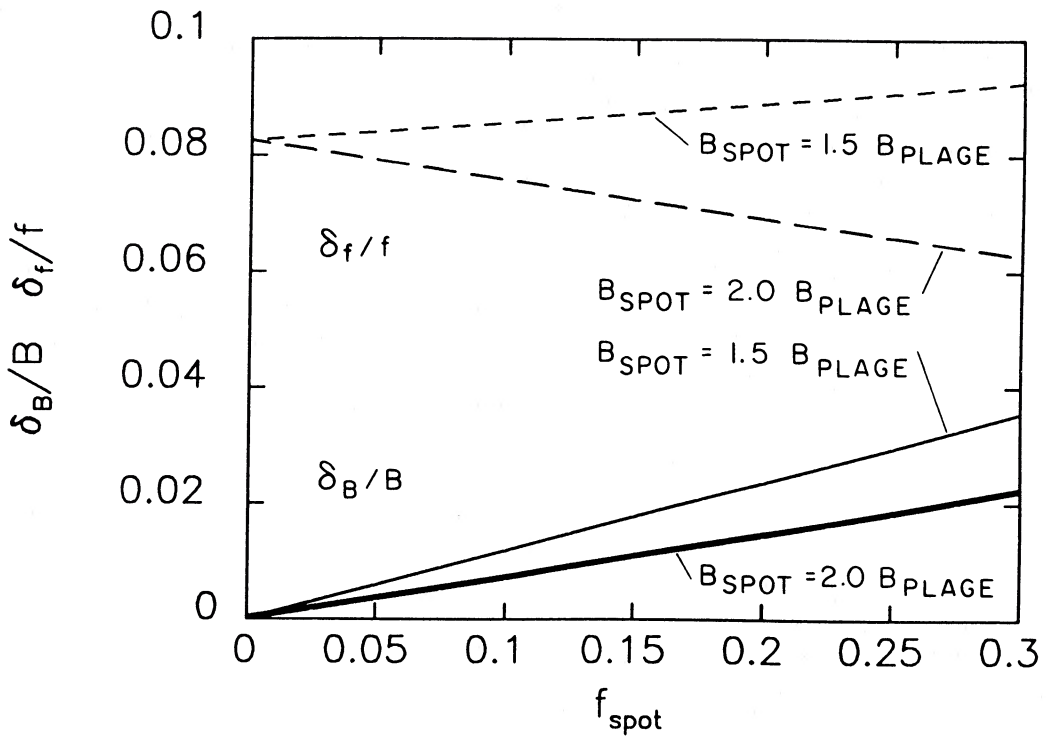

FIG. 13.—Deviations δ_B/B and δ_f/f as a function of f_{spot} and B_{spot} for the multicomponent K star model (see text for details).

1985). It is reasonable, therefore, to ignore the spot contribution to optical lines in most cases since the spot σ component depths would be less than 1% [$R_{spot} f_{spot} F(\lambda_0)(A'/2) \lesssim 0.2 \times 0.2 \times 0.5 \times 0.4$] of the continuum. In the infrared, however, the spot σ components will be nearly 4 times deeper for the same f_{spot}, which could lead to significant systematic errors (SGW) when line profiles are modeled with only two components. When the data warrant, therefore, infrared lines should be modeled with three components: quiet, plage/network, and spot.

For $R_m \neq 1$, the filling factor changes as $1/R_m$. When there is more than one type of magnetic region, but the lines are modeled with $R_m = 1$ and a single value of f, the situation becomes more complex. SGW investigated this problem for lines near 1.5 μm. In a similar analysis, I have taken the "generic" K star line profile with $v \sin i = 5$ km s^{-1} and modified it assuming that both bright plages and dark spots exist on the surface of the model star. The following values were assumed: $B_{spot} = 1.5 B_{plage}$, $T_{plage}/T_{phot} = 1.05$, and $T_{spot}/T_{phot} = 0.70$, and thus R_{plage}(617 nm) = 1.18, R_{plage}(2240 nm) = 1.05, R_{spot}(617 nm) = 0.20, and R_{spot}(2240 nm) = 0.70. The results (Fig. 13) show that only large f_{spot} values affect the f and B values measured using the optical line (δ_f/f is nonzero at $f_{spot} = 0$ because $R_{plage} > 1$). However, even values as small as $f_{spot} \approx 0.10$ cause noticeable changes in f and B determinations using infrared lines (SGW). In addition, many theories suggest that turbulence is suppressed in magnetic regions. Returning to the $R_m \equiv 1$, single magnetic region model for the K star, when $\xi_m = 0.5\xi_{phot}$, the magnetic field parameters derived, assuming $\xi_m = \xi_{phot}$, are $B = 2100$ G and $f = 0.65$, somewhat different from the actual values ($B = 2500$ G and $f = 0.50$). These tests stress the importance of knowing the thermodynamic state of the magnetic atmosphere in order to obtain accurate field strengths and filling factors.

Together with the assumption of uniform properties within the magnetic and quiet regions, the model also assumes a uniform distribution of active regions over the stellar surface. This clearly is not the case for the Sun, and rotational modulation of Ca II flux from many cool stars (Wilson 1978) indicates that their surfaces are similarly inhomogeneous. Very active stars appear to have magnetic areas spread over a wider extent in latitude (Vogt and Penrod 1983; Gilliland 1984), but even these stars certainly are not uniformly covered.

Inhomogeneous coverage of magnetic areas on the stellar surfaces can result in line asymmetries. For example, when the regions of magnetic flux are concentrated at one limb of the star during an observation, the magnetic components of the observed line profile can be shifted by up to $\pm(v \sin i)\lambda/c$. They also will be reduced in strength by foreshortening and limb darkening. Nonuniform active region distributions can be modeled crudely by the addition of a $\pm\Delta\lambda_{region}$ term in the magnetic opacity coefficients. I have chosen to neglect this term for the first-order analyses described here. When a long time series of observations exists, it might be possible to detect active regions rotating on and off the limb (magnetic components migrating through the line profile). Analysis of such data employing a $\pm\Delta\lambda_{region}$ term then would lead to valuable insights concerning the details of the stellar magnetic geometry in a crude form of "magnetic Doppler imaging."

To examine the systematic errors that can arise from neglect of geometric effects, I computed the G star line profile in two extreme configurations: one case in which the active region was concentrated at disk center, and one in which it was evenly split between opposite limbs. The spatial distributions were produced by partitioning Gray's (1976) rotational broadening function for the chosen limb-darkening coefficient into sections in $\Delta\lambda$ appropriate to the spatial configuration and filling factor. The line-of-sight angle, $\langle\gamma\rangle$, used in computing the models also

was adjusted. Though approximate, this approach provides some indication of what extreme spatial configurations could produce. For models with the nominal G star parameters ($B = 1500$ G, $f = 0.30$) with v sin $i = 5$ km s^{-1} and limb active regions, the fit (assuming a normal $\langle\gamma\rangle$) yielded $B = 1500$ G and $f = 0.10$. Disk-center magnetic areas resulted in $B = 1500$ G and $f = 0.60$. These values are roughly consistent with those of Marcy (1982), who used a simpler approach and found errors of $\delta_f \approx 25\%$ and $\delta_B \approx 0\%$. Thus, the topology of magnetic regions on the stellar surface can have a potentially large effect on the perceived filling factor. Only repeated observations of an extremely inhomogeneous star can reveal its true filling factor.

Stellar surface granulation and systematic gas flows in the magnetic regions also can produce asymmetric line profiles. The effects of granulation probably can be ignored, since the maximum velocity difference between line center and the line wing is <0.5 km s^{-1} for main-sequence stars later than F5 (Gray 1982*a*). Similarly, asymmetries due to systematic flows in active regions may be neglected, since the most recent observations of the Sun indicate such (down)flows are <0.1 km s^{-1} (Muller 1985). If, however, unusually strong granulation or enhanced systematic flows do appear in the data, they can be crudely treated by adding a $\pm\Delta\lambda_{\rm flow}$ term to the magnetic σ parameters (Marcy 1982). To test this, a range of flow velocities, between the magnetic and quiet portions of the G star profile, were analyzed (again with no noise) in profile fits with and without first averaging the profile about λ_0. The results suggest δ_B/B from 0 to 0.3 and δ_f/f from 0 to -0.3 can be expected.

Finally, the velocity convolutions used to obtain the stellar flux profile from $I(\lambda)$ are sources of systematic error. The rotational broadening convolution assumes that there are no center-to-limb variations in the line profile, which is strictly valid only when $\beta \gg 1$. While the velocity convolution formulation permits accurate fits to line profiles, it will result in systematic errors in the derived v sin i values for slowly rotating stars. The error, however, is small for v sin $i > 5$ km s^{-1}, and disappears for v sin $i \approx 10$ km s^{-1} (Bruning 1981, 1984). The alternative, a full-disk integration model (Gray 1982*b*; Soderblom 1982), is more realistic but computationally intensive. Because the object of the technique is to obtain accurate *magnetic* parameters for stars, and the convolution method permits good fits to the low-g lines (although not deriving the "correct" v sin i), I have selected the imprecise but speedier convolution method. Future improvements to the model will include a full-disk integration velocity analysis. Similar arguments can be made for the macroturbulence convolution approximation. I use a tabulated radial-tangential macroturbulence function from Gray (1978), which is angle-averaged over the tangential plane and assumes equal radial and tangential velocity dispersions. The use of this approximate, isotropic function undoubtedly introduces some error in the derived macroturbulence, but, again, line profiles can be fitted accurately without resorting to the full-disk integration model. The errors introduced into the derived f and B values by the velocity convolution assumptions should be small.

c) *Effects of Observationally Controllable Factors on the Derived Magnetic Parameters*

The precision of a given magnetic field measurement is dependent on a number of parameters. In this section, I investigate the effects of observationally controllable factors, including the random noise level, the instrumental resolution, line selection (η_0 and λ_0), and star selection (v sin i). To do so, I have defined three "generic" stellar lines (see Table 4) to represent profiles in typical objects that one might observe.

First consider the effects of random Gaussian noise on the detectability and errors in f and B. Synthetic line profiles were generated with the G and K star model parameters using equation (13). Random, Poissonian noise with photon counting statistics (i.e., S/N = flux$^{0.5}$) then was introduced. The resulting profiles were analyzed using equation (13), with all nonmagnetic parameters fixed at the correct values. Thirty synthetic spectra were modeled at each S/N and the results were averaged, yielding mean rms errors in f and B arising from *random noise alone*. Figure 14 displays the normalized errors, $\sigma_B/B \equiv (\langle B_{\rm fit}\rangle - B)/B$ and $\sigma_f/f \equiv (\langle f_{\rm fit}\rangle - f)/f$, for the G star as a function of S/N, together with power-law fits to the results. I find that for both the G and K stars, $\sigma_B/B = c_1(\mathrm{S/N})^{-1.2}$ and $\sigma_f/f = c_2(\mathrm{S/N})^{-1.7}$. In a similar study, Marcy (1982, his Fig. 3) obtained $\sigma_B/B = 0.24$ and $\sigma_f/f = 0.32$ for S/N = 100 and parameters close to those of the G star model. When allowance is made for his use of the observed low-g profile to model the high-g line (increasing the noise by $2^{1/2}$) and use of 20% fewer points per profile, Marcy's results (corrected to $\sigma_B/B = 0.12$ and $\sigma_f/f = 0.16$) compare well with the values of $\sigma_B/B = 0.10$ and $\sigma_f/f = 0.14$ found here.

Although the normalized rms errors in B and f show similar dependences on S/N for the G and K stars, $c_1(\mathrm{G}) > c_1(\mathrm{K})$ and $c_2(\mathrm{G}) > c_2(\mathrm{K})$. This is not surprising, since one intuitively expects that σ_B/B and σ_f/f will increase as the total magnetic flux decreases (fB for the G star is 0.36 times the value for the K star). To investigate the dependence of the errors on the magnetic parameters themselves, I generated model line profiles for the G and M star parameters covering a wide range of f and B. Again, 30 synthetic spectra with random noise were modeled, as above, for each (f, B) pair and averaged. Figures 15 and 16 illustrate contour maps of the errors in the derived magnetic parameters as functions of f and B at various S/N for the G and M star models. It is apparent that the relative errors in f and B depend on both f *and* B. A multilinear regression study of slices through these contours reveals that, to first order, σ_B/B scales as $f^{-1.0}B^{-2.6}$, and σ_f/f scales as $f^{-1.4}B^{-3.4}$. These scaling laws are crude, however, and considerable deviations occur, especially at high filling factors.

A basic difficulty of stellar Zeeman analysis is indicated by the interdependence of the errors in f and B: the derived values of f and B are correlated and difficult to separate uniquely (Marcy 1982; Gray 1984*a*). An examination of the shape of the χ^2 minima for a given fit in the filling factor–magnetic field plane confirms this. The correlation can be understood physically if one assumes optically thin lines and considers the Fourier transform ratio, $F(s)/F_0(s)$, of equation (1) (i.e., the Robinson method; s is the Fourier frequency):

$$\frac{F(s)}{F_0(s)} = 1 - f + f[A' \cos(2\pi\Delta\lambda_B s) + B'] . \quad (18)$$

Then, by expanding in a Taylor series and retaining only first-order terms,

$$\frac{F(s)}{F_0(s)} \approx 1 - fA' + fA'(1 - 2\pi^2\Delta\lambda_B^2 s^2 + \cdots) \propto fB^2 . \quad (19)$$

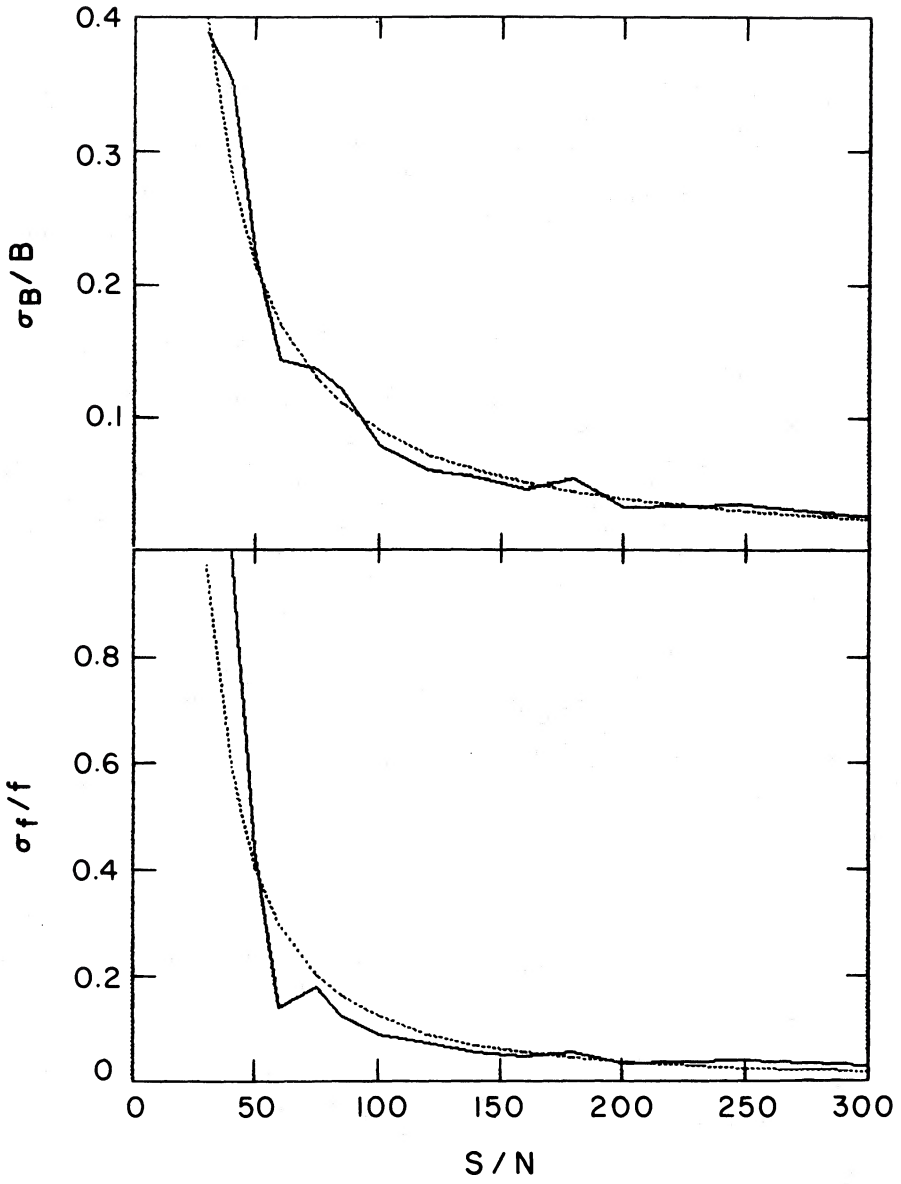

FIG. 14.—Normalized rms errors (*solid curves*) in the magnetic field strength and filling factor, σ_B/B and σ_f/f, as a function of S/N for the G star line parameters (Table 4). The dotted lines are power fits $\sigma_B/B \sim (\mathrm{S/N})^{-1.24}$ and $\sigma_f/f \sim (\mathrm{S/N})^{-1.72}$.

Thus, unless measurements are made to sufficiently high s (i.e., high enough S/N) to see the effects of higher order terms, solutions with fB^2 equal to a constant will be equally preferred. For the same reasons, minima in χ^2 space will be extended roughly along lines of constant fB^2 (e.g., Fig. 2 from Saar and Linsky 1986), and the unique separation of f and B becomes progressively more difficult with decreasing S/N. (As η_0 increases, though, there is a tendency for the exponent to increase as a result of saturation effects: for example, at $\eta_0 = 10$, $fB^{2.3}$ is a constant.) Thus random noise not only limits the accuracy of measurements of f and B directly, but also interferes with the unique separation of the two quantities.

Any process that filters or smooths the line profile also will affect the determinations and separability of the magnetic parameters. Figures 17 and 18 illustrate the errors in f and B for the G and M stars for various rotation rates as functions of the magnetic parameters. For one case investigated in detail (G star; Fig. 19), $\sigma_B/B \sim (v \sin i)^{1.4}$ and $\sigma_f/f \sim (v \sin i)^{1.9}$. Only stars with the largest magnetic fluxes can be accurately measured beyond $v \sin i \approx 12$ km s^{-1} in the optical or $v \sin i \approx 20$ km s^{-1} in the infrared.

Figure 20 illustrates the effect of finite spectral resolution on σ_f/f and σ_B/B for the standard lines and S/N = 100. The errors in σ_B/B scale roughly in proportion to the inverse square of the resolution, $r = \lambda/\Delta\lambda$, as shown by Lites and Skumanich (1984). Power-law fits to the curves yield $\sigma_B/B \sim r^{-1.9}$ and $\sigma_f/f \sim r^{-3.8}$. The wavelength of a line affects magnetic detectability as well. Zeeman broadening becomes more distinguishable at longer wavelengths, since roughly $\Delta\lambda_B/\Delta\lambda_D \sim \lambda_0^{-1}$. A more detailed study confirms this expectation, since σ_B/B and σ_f/f are proportional to λ_0^{-1}.

Line strength also is important to the accuracy of f and B

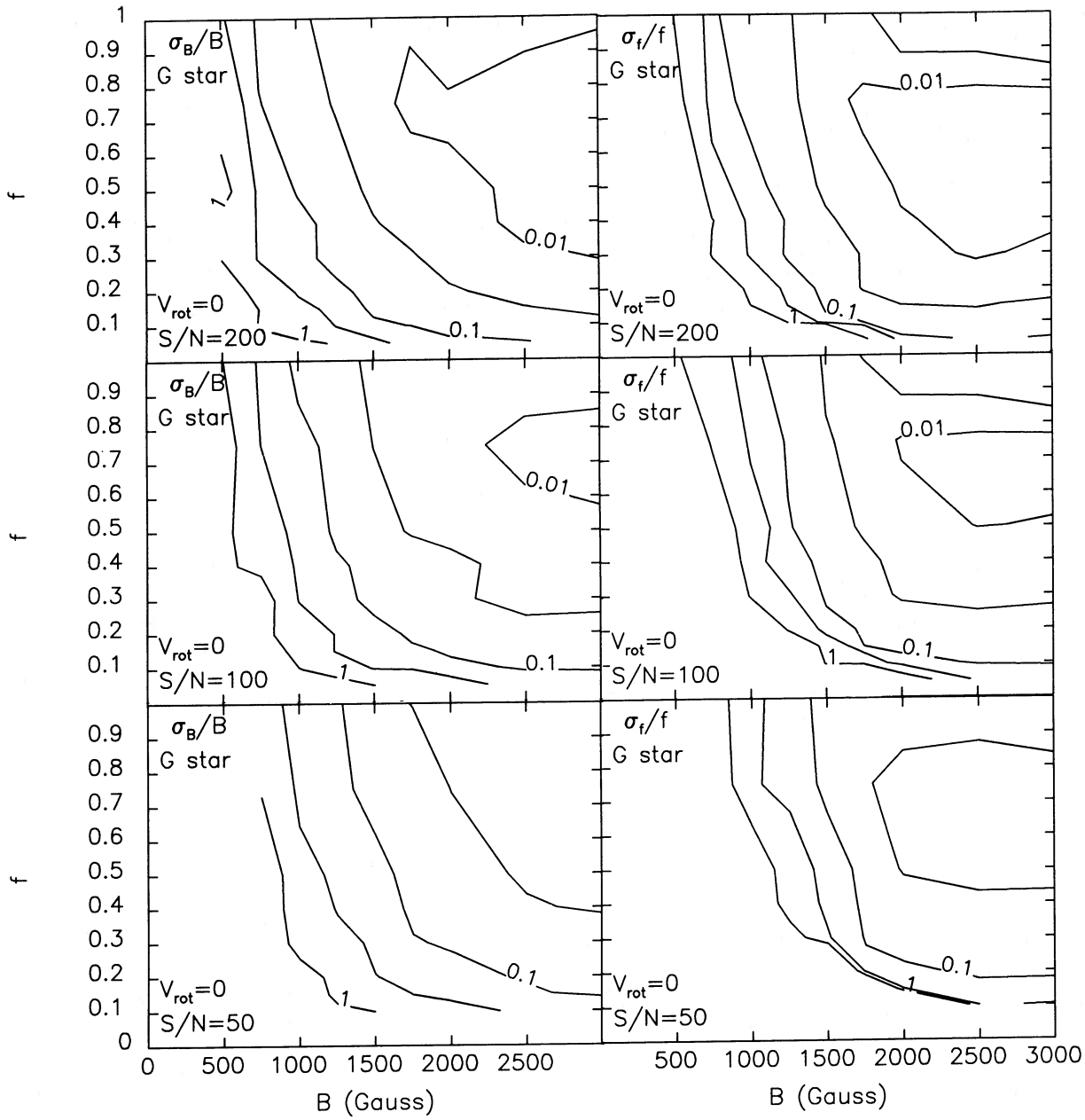

FIG. 15.—Contours of constant rms error, σ_B/B and σ_f/f, for the G star line parameters (here allowing f and B to vary) and imposed S/N ratios of 200, 100, and 50. The contour levels are 0.01, 0.03, 0.1 0.3, and 1.0.

measurements. Weak lines with $\eta_0 \ll 1$ are difficult to use because the absolute profile changes due to magnetic effects are very small. On the other hand, line saturation at $\eta_0 > 1$ begins to smear out the magnetic information through "opacity broadening." Figure 21 depicts the effect of increasing opacity on magnetic flux determinations. I find that the detectability of magnetic fields peaks at $\eta_0 \sim 5$; for larger η_0, the amount of information gained by the increase in the depth of and the number of points in the profile begins to compete with the blurring of information in the increasingly opaque Doppler core. Thus, optimum lines for Zeeman analysis are of intermediate strength, i.e., $1 \lesssim \eta_0 \lesssim 10$: lines on the "knee" of the curve of growth.

V. DISCUSSION AND SUMMARY

A summary of the comparative magnitudes of the various sources of systematic and random error is given in Table 5. In spite of the detailed study undertaken here, it is difficult to calculate the "total" error in any given situation, largely because of difficulties in assessing the overall impact of the systematic errors. The systematic errors are numerous and often quite large; a cursory examination of Table 5 might lead one to conclude that accurate magnetic measurements in late-type stars are nearly impossible. Fortunately, however, many of the systematic errors have mutually canceling effects. The velocity broadening parameters are one example. Generally, ξ

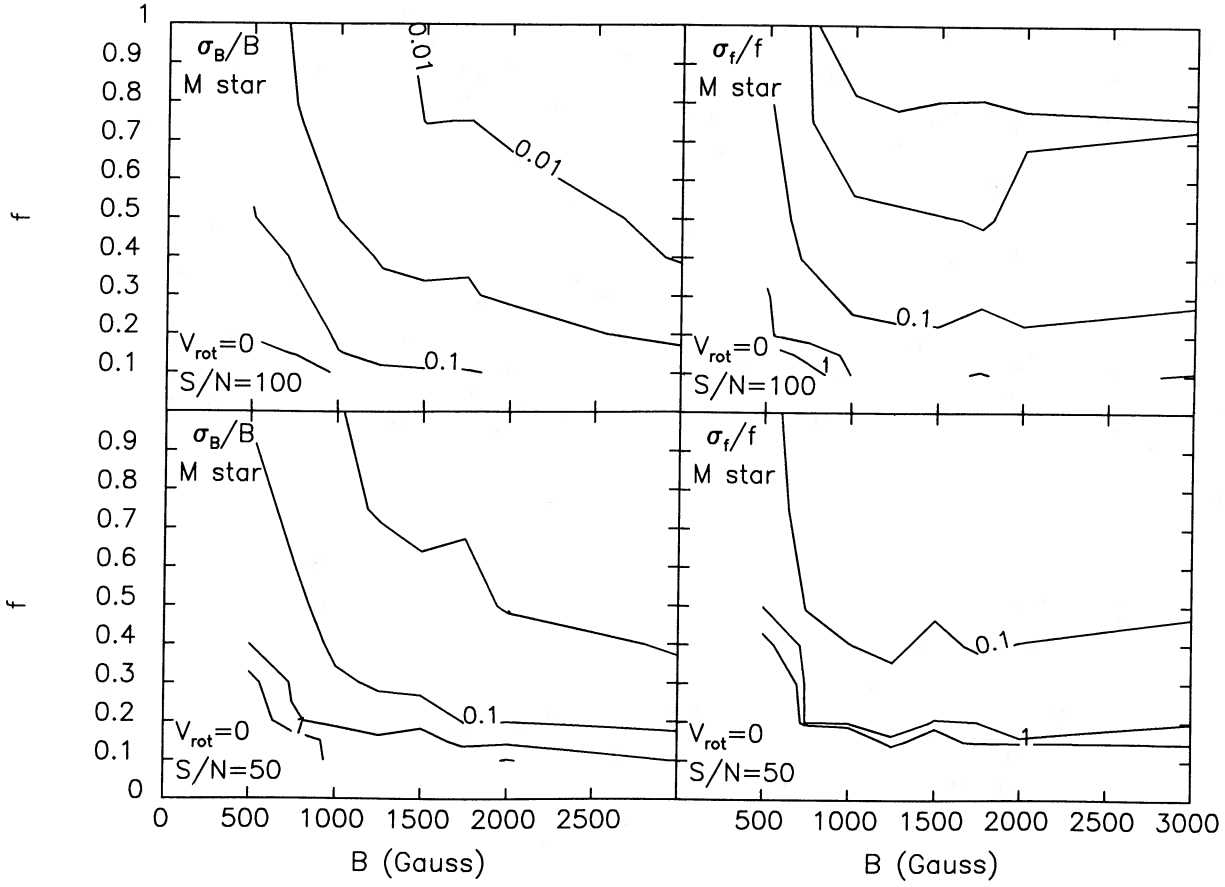

FIG. 16.—Same as Fig. 15, except using the M star line parameters and S/N of 100 and 50

is assumed to be some standard value, and low-g lines are modeled to determine v sin i. If the assumed ξ turns out to be too low, the v sin i derived will be increased to match the total observed line broadening. Since errors in ξ and v sin i act on the magnetic parameters in opposite senses, the net effect on δ_B/B and δ_f/f is minimal. Similarly, if the continuum is defined at too high a level, η_0 will be overestimated and the effects of each on δ_f/f will roughly cancel (the errors in B, however, will slightly increase). Furthermore, the large potential source of error in f resulting from extreme spatial inhomogeneities can be largely eliminated by multiple observations.

To obtain a rough idea of the "total" expected systematic error, I have added the average absolute magnitude of each error in quadrature, and divided the result by 2 (spatial effects were not included in this sum) to account for the aforementioned canceling effects. The results, $\delta_B/B \approx 12\%$ and $\sigma_f/f \approx 28\%$, are large, but not so great as to make stellar magnetic measurements in the optical a hopeless enterprise. Adding these results in quadrature with the random errors (for S/N = 100), one can roughly gauge the total expected error for an individual magnetic field determination using a $g = 2.5$ $\lambda 617$ line: $\delta_B/B \approx 14\%$ and $\delta_f/f \approx 30\%$, ignoring spatial effects. The use of several high-g lines in the analysis will improve these values somewhat, as will repeated observations (which also compensate for unusual magnetic topologies and attendant errors in f). Ultimately, however, the effects of noise and the uncertainty concerning the thermodynamic properties of the stellar active region will be fundamental limiting factors. The stated errors will increase with decreasing f and/or B and decrease for the reverse.

Table 5 also lists the ranges of error in f and B resulting from the neglect of radiative transfer and line-blending effects. These sources of systematic error also must be included when considering measurements by previous methods and by techniques described here that do not compensate fully for line blending. These errors are on the order of the errors discussed above, and larger in some cases. The errors derived for uncompensated blends (Figs. 8 and 10) are roughly consistent with Gray's (1984*a*) estimate of their effect from the magnitude of "anti-Zeeman" broadening that he occasionally saw: $B(A'f)^{0.5} \approx 0.4$; thus for $\langle\gamma\rangle = 43°$, $B = 1500$ G, $f = 0.07$.

These results have numerous implications for stellar Zeeman broadening measurements. First, largely owing to systematic effects, the total expected errors in the magnetic field strength and filling factor probably cannot be held to less than about 25% for optical line profiles. For rapid rotators the problem becomes even worse: at v sin $i = 8$ km s^{-1}, a filling factor of 0.3 for solar-type field strengths becomes essentially undetectable because of the velocity smearing of the magnetic splitting (Fig. 19). Nevertheless, with careful analysis of high S/N profiles, the magnetic parameters of G and K dwarfs can be determined with fair accuracy (total error = 30%–40%) and good precision (random error = 15%–20%) from optical line profiles within the following rough restrictions: for v sin $i = 0$,

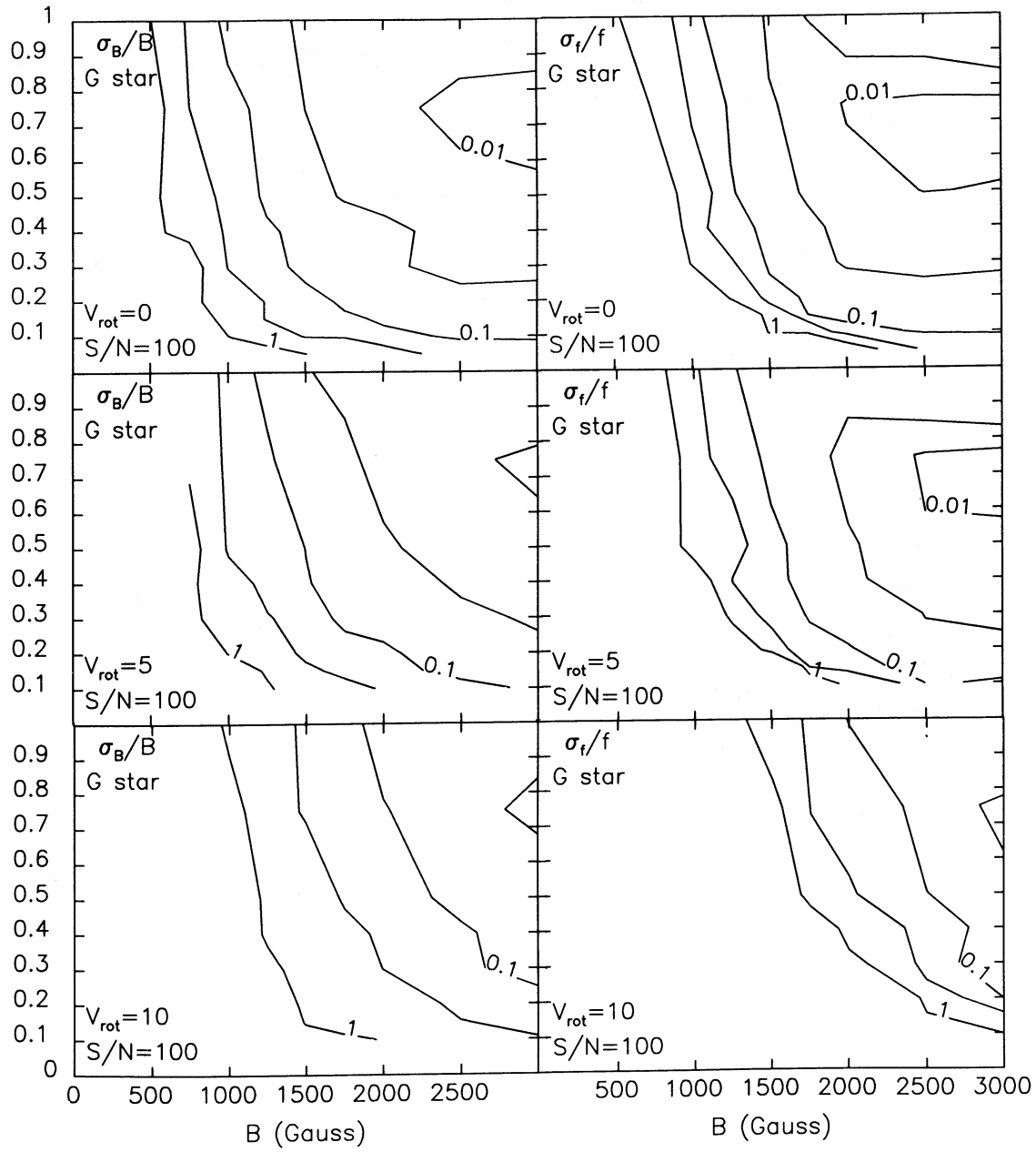

FIG. 17.—Contours of σ_B/B and σ_f/f for the G star model (varying f and B) with $v \sin i = 0$, 5, and 10 km s^{-1}

$f^{1/2}B \gtrsim 700$; for $v \sin i = 5$ km s^{-1}, $f^{1/2}B \gtrsim 850$; and for $v \sin i = 10$ km s^{-1}, $f^{1/2}B \gtrsim 1400$. These limits will permit observations of many interesting objects.

Because of the greater magnetic splitting, stellar Zeeman measurements are more easily made in the infrared. Infrared observations also offer perhaps the only way to observe fields on M dwarf stars, whose optical spectra are heavily blanketed with molecular bands. If field strengths on RS CVn and other active subgiants and giant stars are as small as recent results seem to indicate (500–900 G, Marcy and Bruning 1984; $B \approx 600$ G for λ And, GGB), the infrared might be the only viable region to derive B and f values for these important objects. Unfortunately, only the most slowly rotating giants and subgiants of these classes can be studied, since for $v \sin i = 20$ km s^{-1}, $B \gtrsim 1500$ G and $f \gtrsim 0.35$, roughly, are required for reasonably accurate measurements at 2.2 μm (Fig. 18).

Several improvements and additions can be made to the model described here and how it is employed in actual observing campaigns. A proper, full-disk integration treatment of the rotational and macroturbulent velocities should be included. Better compensation for blends might be possible by synthesizing blend "templates" using detailed model atmosphere calculations of spectra near high-g lines of interest. More realistic model atmospheres might provide better fits to the line profiles. An analysis of asymmetries in low-g lines might provide better understanding of granulation-induced asymmetries that might exist in high-g line profiles. Simultaneous photometry

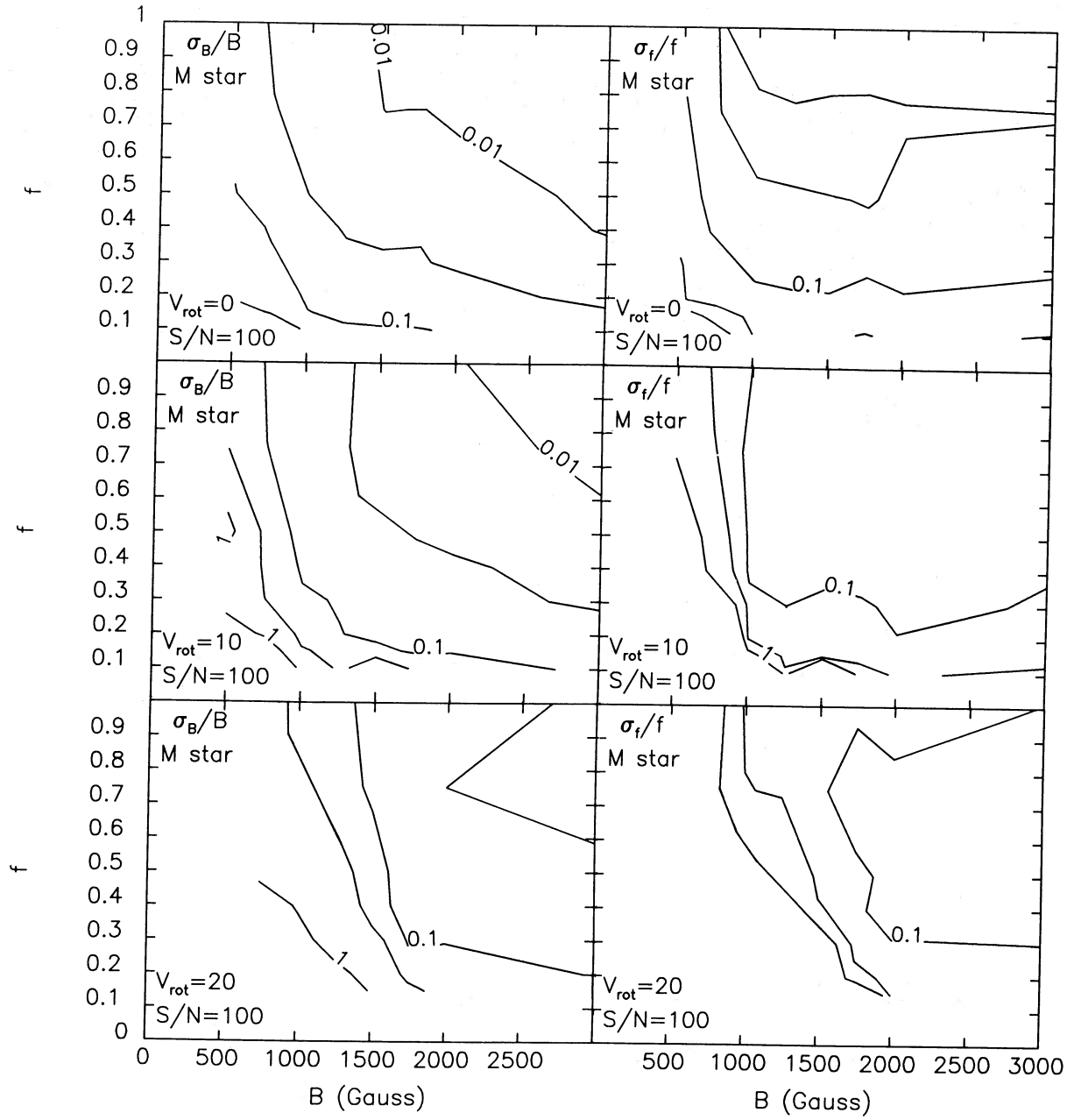

FIG. 18.—Contours of σ_B/B and σ_f/f for the M star model with $v \sin i = 0$, 10, and 20 km s^{-1}

and Doppler imaging could provide constraints on active region properties such as R_m and T_m, and aid in defining the topology of the magnetic regions, thereby reducing sources of systematic error in the model. Estimates of the filling factors for stellar plages from Ca II H and K (LaBonte 1986) or He D_3 λ587.6 nm (Lambert and O'Brien 1983) or for stellar umbrae from Li I λ670.7 nm (Giampapa 1984*b*) or the TiO bands (Ramsey and Nations 1980) could serve as independent checks on f, help separate $f_{\text{plage+network}}$ and f_{spot}, and determine the respective brightness ratios. If typical stellar spot fields are, like the Sun, 1.5–3 times the field strengths in bright stellar magnetic regions, high-resolution, low-noise infrared spectra might show separately resolved spot and plage σ components. Alternatively, one could use optical data to determine the plage magnetic parameters and apply this knowledge to unresolved infrared profiles to extract the values of f and B in spots. Magnetic field strengths and filling factors of both the spot and plage/network areas on active stars could thus be deduced. Measurements of lines formed at different temperatures or heights in the stellar atmosphere could be used to infer the depth dependence of the stellar fields and further probe differences between warm plages and cool spots. Simultaneous linear and circular polarization measurements might help elucidate the details of the magnetic geometry, answering questions concerning the scales over which the fields are bipolar and the inhomogeneity of magnetic regions (see Landi Degl'Innocenti 1982).

In summary, I have developed new techniques for the analysis of magnetic field strengths and filling factors in late-type stellar spectra based on a simple radiative transfer model

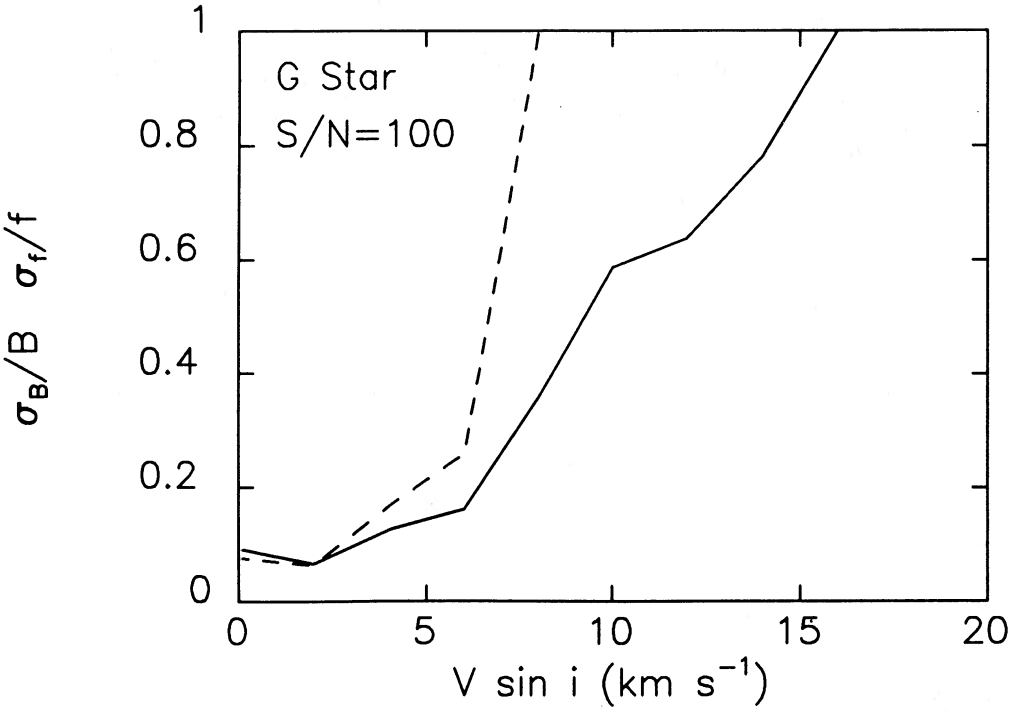

FIG. 19.—Errors σ_B/B (*solid curve*) and σ_f/f (*dashed curve*) for the G star model as a function of v sin i

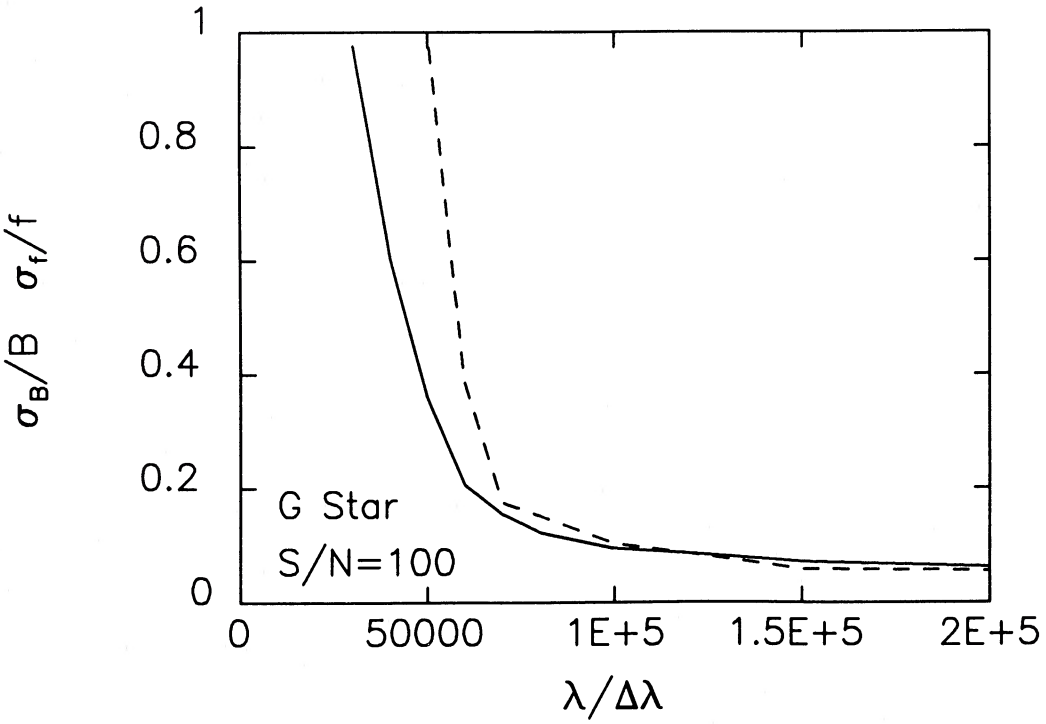

FIG. 20.—Errors σ_B/B (*solid curve*) and σ_f/f (*dashed curve*) for the G star model as a function of resolution, $\lambda/\Delta\lambda$

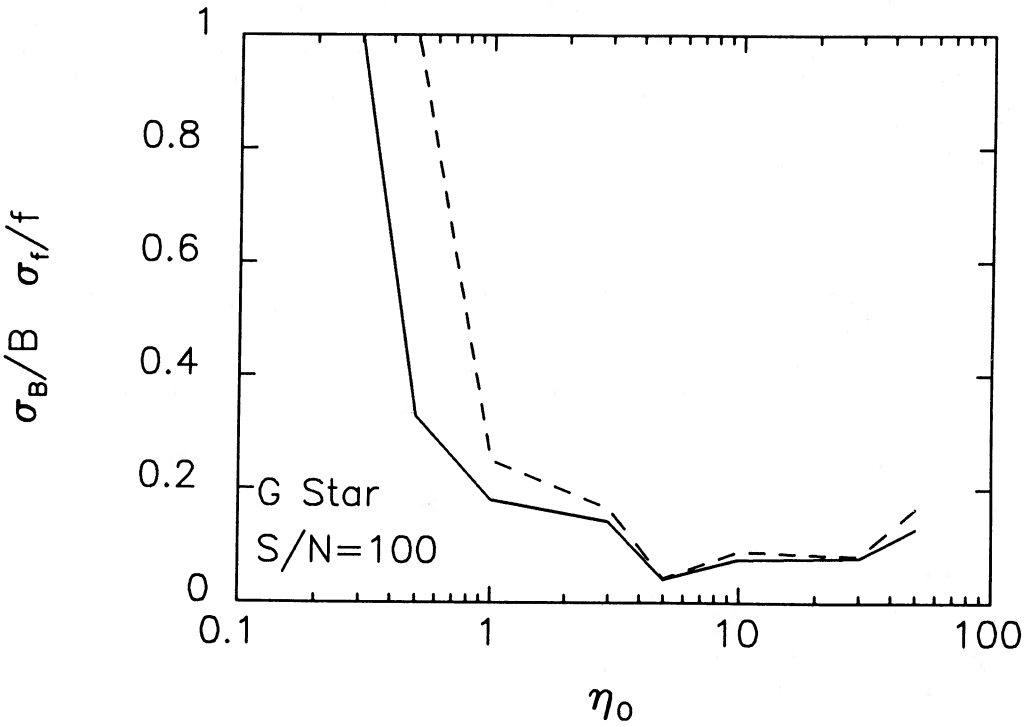

FIG. 21.—Errors σ_B/B (*solid curve*) and σ_f/f (*dashed curve*) for the G star model as a function of η_0

TABLE 5

SUMMARY OF SYSTEMATIC AND RANDOM ERRORS FOR THE G STAR MODEL

A. RANDOM ERRORS

Parameter	Value	σ_B/B	σ_f/f
S/N	200	0.03	0.04
	100	0.07	0.08
	50	0.22	0.35
$v \sin i$ (km s^{-1})	5	0.15	0.22
	10	0.65	>1.00

B. SYSTEMATIC ERRORS

Parameter Error or Test	δ_B/B	δ_f/f
Residual blends	$\begin{cases}+0.20\\-0.10\end{cases}$	$\begin{matrix}0.10\\-0.10\end{matrix}$
$v_{\rm flow} \leq 1$ km s^{-1}	≤ 0.10	≤ -0.15
$\delta_\xi = \pm 0.25$ km s^{-1}	$\begin{cases}+0.12\\-0.10\end{cases}$	$\begin{matrix}-0.35\\+0.40\end{matrix}$
$\delta_\eta/\eta = \pm 0.50$	$\begin{cases}-0.03\\+0.05\end{cases}$	$\begin{matrix}-0.25\\+0.20\end{matrix}$
$\delta_{v \sin i} = \pm 1.5$ km s^{-1}	$\begin{cases}+0.10\\-0.02\end{cases}$	$\begin{matrix}+0.30\\-0.30\end{matrix}$
$\delta_{\rm continuum} = \pm 0.01$	$\begin{cases}-0.15\\+0.02\end{cases}$	$\begin{matrix}+0.18\\-0.05\end{matrix}$
Thermodynamic multiregion effects	<0.20	<0.30
Geometric inhomogeneities	Small	Up to ± 1.00

C. ADDITIONAL SYSTEMATIC ERRORS OF PREVIOUS TECHNIQUES

Source of Error	δ_B/B	δ_f/f
Neglect of saturation ($\eta = 5$)	~ -0.2 to $+0.3$ [a]	~ -0.1 to 0.5 [b]
Blends ($f = 0$)		

[a] $B = 0$–3000.
[b] $f = 0$ to ~ 0.50.

that includes line saturation effects and the full Zeeman patterns. The most accurate of these techniques analyzes line profiles differentially to reduce the influence of weak line blends. I have demonstrated that neglect of such blends and of line saturation effects in previous techniques produces systematic errors in the inferred B and f values. These errors are typically 25%–50%, but in some cases lead to spurious detections. I have parameterized the influence of various observational parameters (such as S/N, η_0, λ_0, $v \sin i$, and resolution) on the derived magnetic field strength and filling factors, and described the effects of random noise on σ_B/B and σ_f/f in detail. Various possible sources of systematic error have also been explored. These were found to dominate the uncertainties in measurements of stellar magnetic fields. It is difficult to reduce errors in f and B below 20% *regardless of the S/N of the data* because of these systematic effects. I have tested techniques developed here by successfully modeling sunspot line profiles and lines from a stellar spectrum (ϵ Eri) with known magnetic parameters. I have also outlined several ideas for improving the model, and discussed useful observational strategies. I conclude that the measurement of stellar magnetic fields and the associated filling factors is a difficult, but not impossible, task.

I would like to thank Dr. Jeff Linsky for encouraging my interest in stellar magnetic fields and for his support throughout. I am also indebted to Dr. Linsky, Dr. D. Bruning, Dr. T. Ayres, Mr. J. Neff, Dr. G. Marcy, and Dr. G. Basri for carefully reading the manuscript and making many constructive comments. Thanks are also due Dr. Marcy for kindly sharing some of his thesis data. It is a pleasure to thank Kitt Peak National Observatory for their generous allocation of telescope time to this project. This research is funded by National Aeronautics and Space Administration grants NGL-06-003-057 and NAG5-82 to the University of Colorado.

REFERENCES

Allen, C. W. 1976, *Astrophysical Quantities* (4th ed.; London: Athlone).
Al-Naimiy, H. M. 1978, *Ap. Space Sci.*, **53**, 181.
Auer, L. H., Heasley, J. N., and House, L. L. 1977, *Solar Phys.*, **55**, 74 (AHH).
Avrett, E. M., and Kurucz, R. L. 1983, *Inst. Theoret. Ap. Oslo Rept.*, No. 59, p. 43.
Ayres, T. R., Marstad, N. C., and Linsky, J. L. 1981, *Ap. J.*, **247**, 545.
Babcock, H. W. 1949, *Ap. J.*, **110**, 126.
———. 1958, *Ap. J. Suppl.*, **3**, 141.
Beckers, J. M. 1969, *A Table of Zeeman Multiplets*, AFCRL-69-0115.
Beckers, J. M., and Schröter, E. H. 1968, *Solar Phys.*, **4**, 142.
Borra, E. F., Edwards, G., and Mayor, M. 1984, *Ap. J.*, **284**, 211.
Brault, J. W., and White, O. R. 1971, *Astr. Ap.*, **13**, 169.
Brown, D. N., and Landstreet, J. D. 1981, *Ap. J.*, **246**, 899.
Bruning, D. H. 1981, Ph.D. thesis, New Mexico State University.
———. 1984, *Ap. J.*, **281**, 830.
Campbell, B., and Cayrel, R. 1984, *Ap. J. (Letters)*, **283**, L17.
Chapman, G. A. 1977, *Ap. J. Suppl.*, **33**, 35.
Dorren, J. D., and Guinan, E. F. 1982, *A.J.*, **87**, 1546.
Eaton, J. C., and Hall, D. S. 1979, *Ap. J.*, **227**, 907.
Frazier, E. N. 1978, *Astr. Ap.*, **64**, 351.
Frazier, E. N., and Stenflo, J. O. 1972, *Solar Phys.*, **27**, 330.
Giampapa, M. S. 1984*a*, in *Stellar Activity and Variability*, ed. F. Praderie and A. Mangeney (Meudon: Université de Paris), p. 309.
———. 1984*b*, *Ap. J.*, **277**, 235.
Giampapa, M. S., Golub, L., and Worden, S. P. 1983, *Ap. J. (Letters)*, **268**, L121 (GGW).
Gilliland, R. L. 1984, in *Cool Stars, Stellar Systems, and the Sun*, ed. S. L. Baliunas and L. Hartmann (New York: Springer), p. 146.
Gondoin, Ph., Giampapa, M. S., and Bookbinder, J. A. 1985, *Ap. J.*, **297**, 710 (GGB).
Gray, D. F. 1976, *The Observation and Analysis of Stellar Photospheres* (New York: Wiley).
———. 1978, *Solar Phys.*, **59**, 193.
———. 1982*a*, *Ap. J.*, **255**, 200.
———. 1982*b*, *Ap. J.*, **262**, 682.
———. 1984*a* *Ap. J.*, **277**, 640.
———. 1984*b*, *Ap. J.*, **281**, 719.
Haisch, B. M. 1983, in *IAU Colloquium 71, Activity in Red Dwarf Stars*, ed. P. B. Byrne and M. Rodonò (Dordrecht: Reidel), p. 255.
Hall, D. N. B. 1973, *An Atlas of Infrared Spectra of the Solar Photosphere and of Sunspot Umbrae* (Tucson: Kitt Peak National Observatory).
Hall, D. N. B., Ridgway, S., Bell, E. A., and Yarborough, J. M. 1979, *Proc. SPIE*, **172**, 121.
Harvey, J. W. 1973, *Solar Phys.*, **28**, 9.
———. 1977, *A Photographic Spectral Atlas of a Sunspot between 3812 and 9182 Å* (Tucson: Kitt Peak National Observatory).
Harvey, J., and Hall, D. 1975, *Bull. A.A.S.*, **7**, 459.
Howard, R., and Stenflo, J. O. 1972, *Solar Phys.*, **22**, 402.
Kjeldseth-Moe, O. 1968, *Solar Phys.*, **4**, 267.
Kurucz, R. L., and Hartmann, L. 1984, SAO preprint, No. 2015.
LaBonte, B. J. 1986, *Ap. J. Suppl.*, **62**, 229.
Lamb, F. K. 1970, *Solar Phys.*, **12**, 186.
Lambert, D. C., and O'Brien, G. T. 1983, *Astr. Ap.*, **128**, 110.
Landi Degl'Innocenti, E. 1982, *Astr. Ap.*, **110**, 25.
Landi Degl'Innocenti, E., and Landi Degl'Innocenti, M. 1973, *Solar Phys.*, **31**, 299.
Landolfi, M., and Landi Degl'Innocenti, E. 1982, *Solar Phys.*, **78**, 355.
Landolfi, M., Landi Degl'Innocenti, E., and Arena, P. 1984, *Solar Phys.*, **93**, 269 (LLA).
Linsky, J. L. 1983, in *IAU Symposium 102, Solar and Stellar Magnetic Fields: Origins and Coronal Effects*, ed. J. O. Stenflo (Dordrecht: Reidel), p. 313.
———. 1985, *Solar Phys.*, **100**, 333.
Lites, B. W., and Cowley, C. R. 1974, *Astr. Ap.*, **31**, 361.
Lites, B. W., and Skumanich, A. 1984, in *Measurements of Solar Vector Magnetic Fields* (NASA Conf. Pub., No. 2374), p. 342.
Livingston, W., and Harvey, J. W. 1969, *Solar Phys.*, **10**, 294.
Marcy, G. W. 1981, *Ap. J.*, **245**, 624.
———. 1982, *Pub. A.S.P.*, **94**, 562.
———. 1984, *Ap. J.*, **276**, 286.
Marcy, G. W., and Bruning, D. H. 1984, *Ap. J.*, **281**, 286.
Muller, R. 1985, *Solar Phys.*, **100**, 237.
Noyes, R. Q., Hartmann, L. W., Baliunas, S. L., Duncan, D. K., and Vaughan, A. H. 1984, *Ap. J.*, **279**, 763.
Poe, C. H., and Eaton, J. A. 1985, *Ap. J.*, **289**, 644.
Pulkovo Akad. Nauk S.S.R. Solar Data Bulletin, No. 4, 1984.
Rachkovskii, D. N. 1961, *Izv. Krymsk. Astrofiz. Obs.*, **25**, 277.
Ramsey, L. W., and Nations, H. L. 1980, *Ap. J. (Letters)*, **239**, L121.
Robinson, R. D. 1980, *Ap. J.*, **239**, 961.
Robinson, R. D., Worden, S. P., and Harvey, J. W. 1980, *Ap. J. (Letters)*, **236**, L155 (RWH).
Rodonò, M., *et al.* 1986, *Astr. Ap.*, **165**, 135.
Rosner, R., Golub, L., and Vaiana, G. S. 1985, *Ann. Rev. Astr. Ap.*, **23**, 413.
Saar, S. H., and Linsky, J. L. 1985, *Ap. J. (Letters)*, **299**, L47.
———. 1986, in *Proc. Fourth Cambridge Workshop on Cool Stars, Stellar Systems, and the Sun*, ed. M. Zeilik and D. M. Gibson (New York: Springer), p. 278.
Saar, S. H., Linsky, J. L., and Beckers, J. M. 1986, *Ap. J.* **302**, 777 (SLB).
Saar, S. H., Linsky, J. L., and Duncan, D. K. 1986, in *Proc. Fourth Cambridge Workshop on Cool Stars, Stellar Systems, and The Sun*, ed. M. Zeilik and D. M. Gibson (New York: Springer), p. 275.
Skumanich, A., Rees, D. E., and Lites, B. W. 1984, in *Measurements of Solar Vector Magnetic Fields* (NASA Conf. Pub. No. 2374), p. 306.
Smith, M. A., and Jaksha, D. B. 1984, in *Proc. Third Cambridge Workshop on Cool Stars, Stellar Systems, and the Sun*, ed. S. L. Baliunas and L. Hartmann (New York: Springer), p. 182.
Soderblom, D. R. 1982, *Ap. J.*, **263**, 239.
———. 1983, *Ap. J. Suppl.*, **53**, 1.
———. 1985, *Pub. A.S.P.*, **97**, 57.
Solanki, S. K., and Stenflo, J. O. 1984, *Astr. Ap.*, **140**, 185.
———. 1985, *Astr. Ap.*, **148**, 123.
Stellmacher, G., and Wiehr, E. 1971, *Solar Phys.*, **18**, 220.
Stenflo, J. O. 1971, in *IAU Symposium 43, Solar Magnetic Fields*, ed. R. Howard (Dordrecht: Reidel), p. 101.
———. 1973, *Solar Phys.*, **32**, 41.
Stenflo, J. O., and Harvey, J. W. 1985, *Solar Phys.*, **95**, 99.
Stenflo, J. O., Harvey, J. W., Brault, J. W., and Solanki, S. 1984, *Astr. Ap.*, **131**, 333.
Stepanov, V. E. 1958, *Izv. Krymsk. Astrofiz. Obs.*, **18**, 136.
———. 1960, *Astr. Zh.*, **37**, 631.
Sun, W.-H., Giampapa, M. S., and Worden, S. P. 1987, *Ap. J.*, **312**, 930 (SGW).
Tarbell, T. D., and Title, A. M. 1977, *Solar Phys.*, **52**, 31.
Unno, W. 1956, *Pub. Astr. Soc. Japan*, **8**, 108.
Vogt, S. S. 1980, *Ap. J.*, **240**, 567.
———. 1983, in *IAU Symposium 71, Activity in Red Dwarf Stars*, ed. P. B. Byrne and M. R. Rodonò (Dordrecht: Reidel), p. 137.
Vogt, S. S., and Penrod, G. D. 1983, *Pub. A.S.P.*, **95**, 565.
Wade, R. A., and Rucinski, S. M. 1985, *Astr. Ap. Suppl.*, **60**, 471.
Walter, F. M., Neff, J. E., Gibson, D. M., Linsky, J. L., Rodonò, M. R., Gary, D. E., and Butler, C. J. 1987, *Astr. Ap.*, in press.
Wiehr, E. 1978, *Astr. Ap.*, **69**, 279.
Wilson, O. C. 1978, *Ap. J.*, **226**, 379.
Zwaan, C. 1986, in *Proc. Fourth Cambridge Workshop on Cool Stars, Stellar Systems, and the Sun*, ed. M. Zeilik and D. M. Gibson (New York: Springer), p. 19.

STEVEN H. SAAR: Smithsonian Astrophysical Observatory, 60 Garden Street, Cambridge, MA 02138